

# Degenerating the complex hyperbolic ideal triangle groups

by

RICHARD EVAN SCHWARTZ

*University of Maryland  
College Park, MD, U.S.A.*

## 1. Introduction

A basic problem in geometry and representation theory is the *deformation problem*. Suppose that  $\varrho_0: \Gamma \rightarrow G_1$  is a discrete embedding of a finitely generated group  $\Gamma$  into a Lie group  $G_1$ . Suppose also that  $G_1 \subset G_2$ , where  $G_2$  is a larger Lie group. The deformation problem amounts to finding and studying discrete embeddings  $\varrho_s: \Gamma \rightarrow G_2$  which extend  $\varrho_0$ .

Let  $\mathbf{H}^2$  be the hyperbolic plane. The complex hyperbolic plane,  $\mathbf{CH}^2$ , is a complex 2-dimensional negatively curved symmetric space which contains  $\mathbf{H}^2$  as a totally real, totally geodesic subspace, and is often considered to be its complexification. The theory of deforming  $\text{Isom}(\mathbf{H}^2)$ -representations into  $\text{Isom}(\mathbf{CH}^2)$ , while quite rich, is still in its infancy. (For a representative sample of such work, see [FZ], [GKL], [GuP], [KR], [To].) The state of affairs is such that one still needs to work out basic examples in detail to gain a foundation for more general considerations.

The *complex hyperbolic ideal triangle groups* are amongst the simplest concrete examples of complex hyperbolic deformations. A complex hyperbolic ideal triangle group is a representation of the form  $\varrho_s: \Gamma \rightarrow \text{Isom}(\mathbf{CH}^2)$ . Here  $\Gamma$  is the free product  $\mathbf{Z}/2 * \mathbf{Z}/2 * \mathbf{Z}/2$ . The representation  $\varrho_s$  maps the standard generators to order-2 complex reflections, such that the product of any two unequal generators is parabolic. (See §2 for definitions.)

There is a real 1-parameter family  $\{\varrho_s \mid s \in \mathbf{R}\}$  of nonconjugate complex hyperbolic ideal triangle groups. The representation  $\varrho_0$  is the complexification of the familiar real ideal triangle group generated by reflections in the sides of an ideal geodesic triangle in the hyperbolic plane. The other representations are deformations.

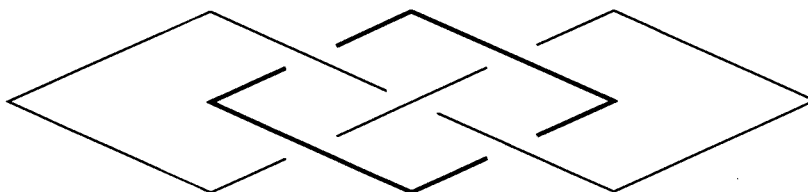


Fig. 1

In [GP], Goldman and Parker studied, and partially classified, which complex hyperbolic ideal triangle groups are discrete and faithful. Let  $g_s$  be the product of all three generators of  $\rho_s(\Gamma)$ , taken in any order. In [S] we proved (and slightly strengthened) the *Goldman–Parker Conjecture*:

**THEOREM [S].**  $\rho_s$  is discrete and faithful if and only if  $g_s$  is not elliptic. Also,  $\rho_s$  is indiscrete when  $g_s$  is elliptic.

The representations  $\rho_s$  and  $\rho_{-s}$  are equivalent after a relabelling of the generators. Thus we think of  $[0, \infty)$  as the space of complex hyperbolic ideal triangle groups. There is a neighborhood of 0 in which  $g_s$  is a hyperbolic element, and there is a neighborhood of  $\infty$  in which  $g_s$  is an elliptic element. The interface between these two intervals is the point  $\bar{s}$  where  $g_{\bar{s}}$  is a parabolic element. We call  $\rho_{\bar{s}}$  the *parabolic representation*.

The theorem above says that all the “business” of the deformation takes place in the vicinity of  $\bar{s}$ . Understanding what happens as  $s \rightarrow \bar{s}$  amounts to understanding the *mechanism of degeneration* for the representations. It is the purpose of this paper to make some progress along these lines.

The unit 3-sphere,  $S^3$ , is the natural ideal boundary of  $\mathbf{CH}^2$ . The *limit set*  $\Lambda_s$  of  $\rho_s(\Gamma)$  is the accumulation set, on  $S^3$ , of any orbit  $\rho_s(\Gamma)(p)$ , where  $p \in \mathbf{CH}^2$ . The definition does not depend on the choice of  $p$ . The *domain of discontinuity* of  $\rho_s(\Gamma)$  is the complement  $\Delta_s = S^3 - \Lambda_s$ .

Let  $\Sigma^3$  denote an abstract copy of the unit 3-sphere  $S^3$ . (We want to distinguish  $\Sigma^3$  from  $S^3$ , to avoid confusion.) Figure 1 shows the Whitehead link  $L$ . From the picture, it is clear that there is a  $(\mathbf{Z}/2 \times \mathbf{Z}/2)$ -symmetry group acting on  $L$ . This symmetry group induces a similar action on the complement  $\Sigma^3 - L$ .

**THEOREM 1.1.** *The quotient  $\Delta_{\bar{s}}/\rho_{\bar{s}}$  is commensurable with the Whitehead link complement. More precisely, let  $\tilde{\Gamma} = \mathbf{Z}/2 * \mathbf{Z}/3$  be the modular group. There is a representation  $\tilde{\rho}_{\bar{s}}: \tilde{\Gamma} \rightarrow \text{Isom}(\mathbf{CH}^2)$  which contains  $\rho_{\bar{s}}$  with index 6. The quotient  $\Delta_{\bar{s}}/\tilde{\rho}_{\bar{s}}(\tilde{\Gamma})$  is homeomorphic to  $(\Sigma^3 - L)/(\mathbf{Z}/2 \times \mathbf{Z}/2)$ , as an orbifold.*

The Whitehead link complement is an example [Th] of a manifold which admits

a complete finite-volume hyperbolic structure. The surprise in our result is that 3-dimensional real hyperbolic geometry appears in a complex hyperbolic setting. As a byproduct of our proof, we give a constructive description of  $\Lambda_{\bar{s}}$ .

To give information near  $\bar{s}$ , we prove

**THEOREM 1.2.** *There is some  $\delta > 0$  having the property: For all  $s \in (\bar{s} - \delta, \bar{s})$ , the groups  $\rho_s(\Gamma)$  and  $\rho_0(\Gamma)$  have topologically conjugate actions on  $S^3$ . In particular,  $\Lambda_s$  is a topological circle and  $\Delta_s/\rho_s(\Gamma)$  is doubly covered by the  $S^1 \times S_2^2$ . Here  $S_2^3$  is the thrice punctured sphere.*

Certainly, Theorem 1.1 should be true for all  $s \in [0, \bar{s})$ . The appearance of  $\delta$  is an artifact of our proof.

In §2 we give background material, and establish a few general preliminary results. In §3 we recall the idea of a *hybrid cone*, defined in [S], and develop it further. In §4 we give a new proof that  $\rho_{\bar{s}}$  is a discrete embedding. In §5 we prove a technical result about the action of the parabolic elements in  $\rho_{\bar{s}}$ . In §6 we characterize  $\Delta_{\bar{s}}$  and  $\Lambda_{\bar{s}}$ . We put everything together in §7, and prove Theorem 1.1. In §8 we prove Theorem 1.2, modulo one detail, which we clear up in §9. The idea in §8 is to show that the analysis in §§4–7 goes through, with suitable changes, for parameters sufficiently close to  $\bar{s}$ .

Though our proofs in the paper do not depend on the computer, we figured out practically every detail in this paper from extensive computer experimentation. In particular, we have programmed every formula of this paper into the computer, and tested it repeatedly.

I would like to thank Martin Bridgeman, Bill Goldman, Jeremy Kahn, Bill Thurston and Justin Wyss-Gallifent for helpful and interesting conversations relating to this work. I would especially like to thank John Parker for many helpful mathematical suggestions.

## 2. Preliminaries

### 2.1. The complex hyperbolic plane

$\mathbf{C}^{2,1}$  is a copy of the vector space  $\mathbf{C}^3$  equipped with the Hermitian form

$$\langle u, v \rangle = u_1 \bar{v}_1 + u_2 \bar{v}_2 - u_3 \bar{v}_3. \quad (1)$$

The spaces  $\mathbf{CH}^2$  and  $\partial\mathbf{CH}^2$  are respectively the projective images, in the complex projective plane  $\mathbf{CP}^2$ , of

$$N_- = \{v \in \mathbf{C}^{2,1} \mid \langle v, v \rangle < 0\} \quad \text{and} \quad N_0 = \{v \in \mathbf{C}^{2,1} \mid \langle v, v \rangle = 0\}. \quad (2)$$

(See [G, p. 67] or [E].) The map

$$\Theta(v_1, v_2, v_3) = \left( \frac{v_1}{v_3}, \frac{v_2}{v_3} \right) \quad (3)$$

takes  $N_-$  and  $N_0$  respectively to the open unit ball and unit sphere in  $\mathbf{C}^2$ . Henceforth we identify  $\mathbf{CH}^2$  with the open unit ball.

Given a point  $V \in \mathbf{CH}^2 \cup S^3$ , we will say that  $\tilde{V} \in \Theta^{-1}(V)$  is a *lift* of  $V$ , and that a lift of the form  $(v_1, v_2, 1)$  is *affinely normalized*. We define the *vector*  $\Theta^{-1}(V)$  as the affinely normalized lift of  $V$ .

$SU(2, 1)$  is the group of  $\langle \cdot, \cdot \rangle$ -preserving, determinant-1 complex linear transformations.  $PU(2, 1)$  is the projectivization of  $SU(2, 1)$ , and elements of  $PU(2, 1)$  preserve  $\mathbf{CH}^2$ . Concretely, each  $\tilde{T} \in SU(2, 1)$  determines an element of  $PU(2, 1)$  via

$$T = \Theta \circ \tilde{T} \circ \Theta^{-1}. \quad (4)$$

The map  $\tilde{T} \rightarrow T$  is a three-to-one surjective Lie group homomorphism.

An element  $T \in PU(2, 1)$  is called *loxodromic* if  $T$  has exactly two fixed points in  $S^3$ , *parabolic* if it has exactly 1 fixed point in  $S^3$ , and *elliptic* if it has a fixed point in  $\mathbf{CH}^2$ . This classification is exhaustive and exclusive.  $T$  is called *ellipto-parabolic* if  $T$  is parabolic and also stabilizes a complex line in  $\mathbf{CP}^2$ . (See [G, p. 203] for more details.) For instance, the element  $g_{\bar{s}}$  is ellipto-parabolic.

Up to scale, there is a unique Riemannian metric on  $\mathbf{CH}^2$  which is invariant under  $PU(2, 1)$ . This metric is the real part of a Kähler metric. It is known as the *complex hyperbolic metric*.

## 2.2. Heisenberg space

We call  $\mathcal{H} = \mathbf{C} \times \mathbf{R}$  *Heisenberg space*, and we call  $H_0 = \{0\} \times \mathbf{R}$  the *center* of Heisenberg space. Given  $p \in S^3$ , a *Heisenberg stereographic projection from  $p$*  is a transformation  $\mathbf{B}: S^3 - \{p\} \rightarrow \mathcal{H}$  of the form

$$\mathbf{B} = \pi \circ \beta, \quad \pi(z, w) = (z, \operatorname{Im}(w)). \quad (5)$$

Here  $\beta$  is a complex projective transformation of  $\mathbf{CP}^2$  which identifies  $\mathbf{CH}^2$  with the *Siegel domain*

$$\{(z, w) \mid \operatorname{Re}(w) > |z|^2\} \subset \mathbf{C}^2 \subset \mathbf{CP}^2. \quad (6)$$

We write  $\infty = \mathbf{B}(p)$  in this case.  $\mathbf{B}$  conjugates the  $PU(2, 1)$ -stabilizer of  $p$  to *Heisenberg automorphisms* of  $\mathcal{H}$ .

Heisenberg automorphisms are real affine maps having the form

$$F(z, t) \rightarrow (f_1(z), f_2(z, t)). \quad (7)$$

Here  $f_1(t)$  is either a complex affine map, or the composition of complex conjugation with a complex affine map. We say that  $F$  covers  $f_1$ . The set of all Heisenberg automorphisms is generated by maps of the following type:

$$F(z, t) = (z + \lambda, t + 2\operatorname{Im}(\bar{\lambda}z) + s), \quad \lambda \in \mathbf{C}, s \in \mathbf{R}, \quad (8)$$

$$F(z, t) = (\lambda z, |\lambda|^2 t + s), \quad \lambda \in \mathbf{C}^*, s \in \mathbf{R}. \quad (9)$$

If  $F$  and  $G$  are Heisenberg automorphisms which both cover the same map then there is some  $s \in \mathbf{R}$  such that  $G(z, t) = F(z, t) + (0, s)$ .

The complex lines tangent to  $S^3$  form a canonical contact distribution  $\mathcal{E}$  on  $S^3$ . Heisenberg stereographic projection maps  $\mathcal{E}$  to a corresponding distribution in  $\mathcal{H}$ , which we give the same name. In  $\mathcal{H}$ , the distribution  $\mathcal{E}$  is the null distribution to the contact form

$$\omega = 2y dx - 2x dy + dt. \quad (10)$$

(See [G, p. 124].) Here  $\mathbf{C}$  has been identified with  $\mathbf{R}^2$  in the usual way.  $\mathcal{E}$  has cylindrical symmetry, in that it is invariant under the maps from equation (9).

We say that a curve is *CR-horizontal* if its tangent vector, at every point, is contained in  $\mathcal{E}$ . The *vertical projection*  $\pi_{\mathbf{C}}(z, t) = z$  is a fibration from  $\mathcal{H}$  to  $\mathbf{C}$ . If  $\gamma: \mathbf{R}/\mathbf{Z} \rightarrow \mathbf{C}$  is a piecewise smooth closed loop and  $t \in \mathbf{R}$  then there is a unique CR-horizontal lift  $\tilde{\gamma}: [0, 1] \rightarrow \mathcal{H}$  such that  $\pi_{\mathbf{C}} \circ \tilde{\gamma} = \gamma$  and  $\tilde{\gamma}(0) = t$ . The *monodromy* is  $\tilde{\gamma}(1) - \tilde{\gamma}(0) = (0, A)$ , where  $A$  is proportional to the signed area of the region bounded by  $\gamma$ . This well-known result follows from equation (10) and from Green's Theorem.

Here is a useful consequence of equation (10): If  $\Pi$  is a plane in  $\mathcal{E}$ , based at the point  $(z, t)$ , then the maximum slope of a vector in  $\Pi$  is  $2|z|$ . (The slope of a vector  $(z, t)$  is defined as  $\pm t/|z|$ .)

### 2.3. Special curves

**2.3.1. Complex slices and C-circles.** A *complex slice* is the intersection of a complex line in  $\mathbf{CP}^2$  with  $\mathbf{CH}^2$ . Complex slices are totally geodesic subspaces, when considered as Riemannian subspaces of  $\mathbf{CH}^2$ .

A *C-circle* (also known as a *chain*) is the ideal boundary, on  $S^3$ , of a complex slice. A C-circle is a round circle, being the intersection of a complex line with  $S^3$ . The C-circles are everywhere transverse to  $\mathcal{E}$ . A *C-arc* is a nontrivial arc of a C-circle. Given two points  $p \neq q \in S^3$ , there is a unique C-circle containing  $p$  and  $q$ .

Let  $N_+ = \mathbf{C}^{2,1} - N_- - N_0$ . If  $C$  is a  $\mathbf{C}$ -circle, then there is the *polar vector*  $C^* \in N_+$ , unique up to scaling, such that  $C = \{v \in N_0 \mid \langle v, C^* \rangle = 0\}$ . There is a unique involution  $I_C \in PU(2, 1)$  fixing  $C$ . As in [G, p. 70], this map is computed by setting  $I_C = \Theta \circ I_{C^*} \circ \Theta^{-1}$ , where

$$I_{C^*}(\tilde{u}) = -\tilde{u} + \frac{2\langle \tilde{u}, C^* \rangle}{\langle C^*, C^* \rangle} C^*. \quad (11)$$

A *Heisenberg  $\mathbf{C}$ -circle* (also called a *Heisenberg chain*) is the image of a chain under a Heisenberg stereographic projection. The curves  $(\{z\} \times \mathbf{R}) \cup \infty$  are chains. In particular, the center of  $\mathcal{H}$  is a chain (with  $\infty$  deleted). All other Heisenberg chains are ellipses which project to round circles under projection  $\pi_{\mathbf{C}}: \mathcal{H} \rightarrow \mathbf{C}$ . (See [G, p. 125].) Let  $C$  be such a chain, with center of mass  $c$ . We have  $C \subset E_c$ , where  $E_c$  is the affine plane which is tangent to  $\mathcal{E}$  at  $c$ . We will say that a *round* Heisenberg chain is one which is, itself, a round circle. The center of mass of a Heisenberg chain is contained in the center of  $\mathcal{H}$  if and only if the chain is round. Such curves are contained in planes of the form  $\mathbf{C} \times \{t\}$ .

**2.3.2. Real slices and  $\mathbf{R}$ -circles.** A *real slice* is a totally real, totally geodesic subspace of  $\mathbf{CH}^2$ . Every real slice is isometric to the real slice  $\mathbf{R}^2 \cap \mathbf{CH}^2$ . An  $\mathbf{R}$ -circle is the ideal boundary, in  $S^3$ , of a real slice. Every  $\mathbf{R}$ -circle is  $PU(2, 1)$ -equivalent to the particular  $\mathbf{R}$ -circle  $\mathbf{R}^2 \cap S^3$ . All  $\mathbf{R}$ -circles are CR-horizontal. An  *$\mathbf{R}$ -arc* is a nontrivial arc of an  $\mathbf{R}$ -circle. There is more than one  $\mathbf{R}$ -arc joining two points in  $S^3$ . We will have more to say about this in the section below on spinal spheres.

A *Heisenberg  $\mathbf{R}$ -circle* is the image of an  $\mathbf{R}$ -circle under a Heisenberg stereographic projection. Any Heisenberg  $\mathbf{R}$ -circle  $\gamma$  which contains  $\infty$  is (the extension of) a straight line. We call these  $\mathbf{R}$ -circles *straight*.  $\gamma$  has the form  $(L \times \{t\}) \cup \infty$  where  $L \in \mathbf{C}$  is a line through the origin, if and only if  $\gamma$  is straight and intersects the center of  $\mathcal{H}$ . In this case we call  $\gamma$  *level*. All other Heisenberg  $\mathbf{R}$ -circles are curves, which project to lemniscates via  $\pi_{\mathbf{C}}$ . One such lemniscate is given in polar coordinates by  $r^2 = \cos(2\theta)$ . All other lemniscates are equivalent to this one by complex affine maps. (See [G, p. 139].)

## 2.4. Cylindrical projection

We define the *cylindrical projection*

$$\xi(z, t) = \{(\arg z, t)\}, \quad z \neq 0; \quad \xi(0, t) = \mathbf{R}/2\pi\mathbf{Z} \times \{t\}.$$

$\xi$  maps the point  $p \in \mathcal{H}$  to the subset  $\xi(p)$  of the flat cylinder  $\Xi = \mathbf{R}/2\pi\mathbf{Z} \times \mathbf{R}$ . When  $p$  is not in the center, we can interpret  $\xi(p)$  as a point.

The following technical result will be used in §4.3.

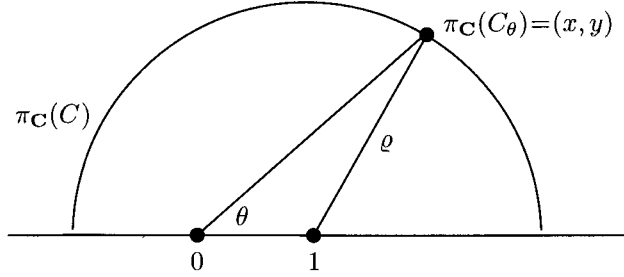


Fig. 2

LEMMA 2.1. *Let  $C$  be an elliptical Heisenberg chain which links the center and which is not round. Let  $c$  be the center of mass of  $C$ , and let  $\varrho$  be the radius of  $\pi_{\mathbf{C}}(C)$ . Then  $\xi(C)$  is the graph of the function  $g(\theta - \theta_0) + B$ , where*

$$g(\theta) = A \sin(\theta) (\cos(\theta) + \sqrt{E + \cos^2(\theta)}),$$

$$A = 2|\pi_{\mathbf{C}}(c)|^2, \quad B = \pi_{\mathbf{R}}(c), \quad E = (\varrho/|\pi_{\mathbf{C}}(c)|)^2 - 1, \quad \theta_0 = \angle(0\overrightarrow{\pi_{\mathbf{C}}(c)}, \mathbf{R}^+).$$

*Proof.* Let  $C_\theta$  be the point on  $C$  such that  $\pi_{\mathbf{C}}(C_\theta)$  makes an angle  $\theta$  with the positive real axis.  $\xi(C)$  is the graph of the function  $\theta \rightarrow \pi_{\mathbf{R}}(C_\theta)$ . To compute this function, we first normalize as much as possible, by maps from equation (9).

Applying the map  $(z, t) \rightarrow (z, t - B)$ , we can assume without loss of generality that  $B = 0$ . Applying a rotation  $(z, t) \rightarrow (uz, t)$  by  $-\theta_0$  about the center we can assume without loss of generality that  $\theta_0 = 0$ . We now have  $c = (+\sqrt{A/2}, 0)$ . Applying the map  $(z, t) \rightarrow (z\sqrt{2/A}, 2t/A)$  we get  $c = (1, 0)$  and  $A = 2$ . The quantity  $E$  is not changed by any of these normalizations.

We set  $(x, y) = \pi_{\mathbf{C}}(C_\theta)$ . (See Figure 2.) We have  $\pi_{\mathbf{R}}(C_\theta) = 2y$ . Our formula comes from solving the equations

$$(x - 1)^2 + y^2 = \varrho^2, \quad x = y \cot(\theta)$$

in terms of  $y$ . □

## 2.5. The cross ratio

Given four distinct points  $x_1, x_2, x_3, x_4 \in S^3$  we define the *Korányi–Reimann cross ratio*

$$\mathbf{X}(x_1, x_2, x_3, x_4) = \frac{\langle X_3, X_1 \rangle \langle X_4, X_2 \rangle}{\langle X_4, X_1 \rangle \langle X_3, X_2 \rangle}. \quad (12)$$

Here  $X_j$  is a null lift of  $x_j$ . One can easily see that the cross ratio is independent of lift, and invariant under the action of  $PU(2, 1)$ . Aside from the specific formula, these are the only properties of the cross ratio we will use. Some additional properties are summarized in [G, §7.2].

## 2.6. Spinal spheres

For information about spinal spheres, see [G, §5]. Here are some equivalent definitions of spinal spheres:

- (1) A spinal sphere is the union of all  $\mathbf{R}$ -arcs containing two fixed points in  $S^3$ .
- (2) A spinal sphere is any inverse image, under Heisenberg stereographic projection, of  $(\mathbf{C} \times \{0\}) \cup \infty$ .
- (3) A *bisector* is the locus of points equidistant from two distinct points in  $\mathbf{CH}^2$ . A spinal sphere is the accumulation set, in  $S^3$ , of a bisector.
- (4) The orthogonal projection onto a complex slice extends to  $S^3$ . A spinal sphere is the inverse image of a geodesic, contained in a complex slice, under orthogonal projection to that slice.

As suggested by our first definition, a spinal sphere has a singular foliation by  $\mathbf{R}$ -arcs. These  $\mathbf{R}$ -arcs are disjoint except for two points, which are called the *poles* of the spinal sphere. The  $\mathbf{C}$ -circle joining the poles is called the *spine* of the spinal sphere. The spine intersects the sphere only at the poles. Spinal spheres have a second singular foliation by chains. Again, the poles are the singular points. These two singular foliations look respectively like lines of longitude and latitude on a globe.

## 3. Hybrid spheres

§§3.1–3.4 also appear in [S], with minor changes. The material in §§3.5–3.7 is new. On the first pass, the reader might want to skip the material in §§3.5–3.7, which is not used until §8.

### 3.1. Parabolic hybrid cones

We say that a *flag* is a pair  $(E, p)$ , where  $E$  is a chain and  $p \in E$  is a point.

LEMMA 3.1. *Suppose  $X \in S^3 - E$ . There is a unique  $\mathbf{R}$ -circle  $\gamma = \gamma(E, p; X)$  such that  $X \in \gamma$  and  $p \in \gamma$ ,  $\gamma \cap (E - p) \neq \emptyset$ .*

*Proof.* We normalize by a Heisenberg stereographic projection so that  $E = H_0$ , the center of  $\mathcal{H}$ , and  $p = \infty$ . In this case, there is a unique level Heisenberg  $\mathbf{R}$ -circle containing  $X$ . This is  $\gamma(H_0, \infty; X)$ .  $\square$

Let  $\Omega(E, p; X)$  be the portion of  $\gamma$  which connects  $p$  to  $X$  but which avoids  $E - p$ . (See Figure 3.) Given a set  $S \subset S^3 - E$ , we define

$$\Omega(E, p; S) = \bigcup_{X \in S} \Omega(E, p; X).$$



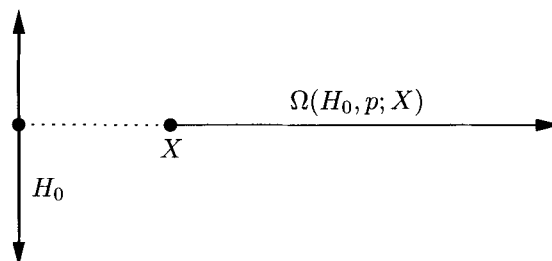


Fig. 3

We call  $\Omega$  the *parabolic hybrid cone*. When the context is clear, we will call  $\Omega$  a *hybrid cone*, as we did in [S]. Our construction is natural. The  $PU(2, 1)$ -image of a hybrid cone is again a hybrid cone.

We say that  $\Omega(E, p; S)$  is in *standard position* if, as in Lemma 3.1, it is normalized so that  $E$  is the center of  $\mathcal{H}$  and  $p = \infty$ .

### 3.2. Parabolic hybrid spheres

Let  $(E, p)$  be a flag, and let  $C$  be a chain which links  $E$ . We define the *parabolic hybrid sphere*

$$\Sigma(E, p; C) = \Omega(E, p; C) \cup I_C(\Omega(E, p; C)),$$

where  $I_C$  is the complex reflection in  $C$ . Here is some additional terminology:

- (1)  $C$  is the *equator* of  $\Sigma$ .
- (2) The flags  $(E, p)$  and  $(I_C(E), I_C(p))$  are the *spines* of  $\Sigma$ .
- (3) The points  $p$  and  $I_C(p)$  are the *poles* of  $\Sigma$ .
- (4)  $\Omega(E, p; C)$  and  $I_C(\Omega(E, p; C))$  are the *hemispheres* of  $\Sigma$ .

A hybrid sphere is determined by its equator and spines.

Say that a *piecewise analytic embedded sphere* (resp. *disk*) is the image of a continuous embedding  $\psi: \Sigma \rightarrow S^3$ . Here  $\Sigma$  is a 2-sphere (resp. disk) with a finite analytic cell division, and  $\psi$  is analytic when restricted to each open cell of  $\Sigma$ .

LEMMA 3.2.  $\Sigma(E, p; C)$  is a *piecewise analytic sphere*.

*Proof.* We will show that the hemispheres are piecewise analytic embedded disks, which intersect exactly along the equator. If two piecewise analytic disks share a common boundary, and intersect only along this boundary, their union is a piecewise analytic sphere.

We normalize so that  $\Omega = \Omega(E, p; C)$  is in standard position. Here  $C$  is an ellipse which links  $E$ . The map  $\xi(z, t) = (\arg z, t)$  is injective and analytic on  $C$ , and is a fibration

from  $(\mathbf{C}-\{0\})\times\mathbf{R}$  onto an infinite cylinder.  $\Omega(E, p; C)$  is obtained from  $C$  by gluing on rays which are subsets of the fibers of the fibration. From this description it is clear that  $\Omega(E, p; C)$  is embedded, and analytic away from  $\{p\}\cup C$ . We arbitrarily choose points  $X_1, X_2 \in C$ . Let  $C_1$  and  $C_2$  be the two arcs of  $C$  bounded by  $X_1$  and  $X_2$ . Let  $\Omega_j = \Omega(E, p; C_j)$ . We can write  $\Omega = \Omega_1 \cup \Omega_2$ , where  $\Omega_1 \cap \Omega_2 = \Omega(E, p; X_1 \cup X_2)$  is a union of two analytic arcs. This structure shows that  $\Omega$  is a piecewise analytic disk.

Let  $\pi_{\mathbf{C}}: \mathbf{C} \times \mathbf{R} \rightarrow \mathbf{C}$  be projection. Recall that  $I_C$  is the involution with fixed point set  $C$ . It follows from symmetry that  $I_C$  maps the exterior of the cylinder  $\Lambda_C = \pi_{\mathbf{C}}^{-1}(C)$  into the interior. Thus  $I_C(\Omega - C)$  and  $\Omega - C$  lie in different components of  $\Lambda_C$ , so that  $\Omega \cap I_C(\Omega) = C$ .  $\square$

### 3.3. Eccentricity

We use the notation from the previous section. We say that  $\Sigma$  is in standard position if one of its hemispheres,  $\Omega(E, p; C)$ , is in standard position. In this case,  $S_C = \pi_{\mathbf{C}}(C)$  is a round circle in  $\mathbf{C}$ , which bounds a disk  $\Delta_C \subset \mathbf{C}$ . The linking condition implies that  $0 \in \Delta_C - S_C$ .

Let  $c$  and  $\rho$  be the center and radius of  $\Delta_C$ . We define the *eccentricity* of  $\Sigma(E, p; C)$  to be the ratio

$$e(\Omega) = e(C) = |c|/\rho. \quad (13)$$

The quantity in equation (13) does not change if we apply to  $\Sigma$  one of the maps from equation (9). Thus, we can define the eccentricity of an arbitrary hybrid sphere by first moving it to standard position and then computing. This definition still requires a choice of hemisphere. By symmetry, both hemispheres give the same answer.

**LEMMA 3.3.** *Two parabolic hybrid spheres are  $PU(2, 1)$ -equivalent if and only if they have the same eccentricity.*

*Proof.* The “only if” direction follows from the well-definedness of the eccentricity. Now for the “if” direction. For  $j=1, 2$ , let  $\Omega_j = \Omega(E_j, p_j; C_j)$  be a standard position hemisphere of the hybrid sphere  $\Sigma_j$ . Normalizing by maps from equation (9), we can arrange that  $C_j$  intersects  $\mathbf{R} \times \{0\}$  in points  $(1, 0)$  and  $(e_j, 0)$ , where  $e_j \in [-1, 0)$ . The center of  $\pi_{\mathbf{C}}(C_j)$  is  $\frac{1}{2}(1+e_j)$ , and the radius is  $\frac{1}{2}(1-e_j)$ . The eccentricity of  $\Sigma_j$  is therefore  $(1+e_j)/(1-e_j)$ . If  $\Sigma_1$  and  $\Sigma_2$  have the same eccentricity then  $e_1 = e_2$ . Since chains are determined by two points,  $C_1 = C_2$ . Since  $\Omega_1$  and  $\Omega_2$  are in standard position,  $\Omega_1 = \Omega_2$ . Finally,  $\Sigma_1 = \Sigma_2$  as well.  $\square$

*Remark.* If  $\Sigma$  has eccentricity 0 then we can normalize so that the hemisphere  $\Omega(E, p; C)$  is in standard position, and so that  $C = S^1 \times \{0\}$ . In this case,  $\Sigma(E, p; C) =$

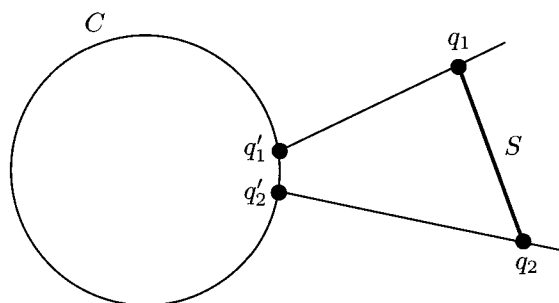


Fig. 4

$(\mathbf{C} \times \{0\}) \cup \infty$ . Hence, a spinal sphere is a parabolic hybrid sphere of eccentricity 0. One can think of the eccentricity as a measure of how far a hybrid sphere deviates from a spinal sphere.

As an alternate formulation, one could say that a hybrid sphere is a spinal sphere if and only if its two spines share a common chain.

### 3.4. Complex tangencies

Recall that  $\mathcal{E}$  is the contact plane field on Heisenberg space. The plane  $\mathbf{C} \times \{0\}$  has the following feature: For any nonzero  $z \in \mathbf{C}$  the plane of  $\mathcal{E}$ , based at  $(z, 0)$ , does not coincide with the tangent plane to  $\mathbf{C} \times \{0\}$  at  $(z, 0)$ .

We say that a hybrid sphere (or hemisphere) is *tame* if its eccentricity is less than  $\frac{1}{2}$ .

LEMMA 3.4. *Suppose that  $\Omega(E, p; C)$  is a tame hybrid hemisphere, and that  $q \in \Omega - p$ . The tangent plane to  $\Omega$  at  $q$  does not coincide with the contact plane at  $q$ .*

*Proof.* We may assume that  $\Omega(E, p; C)$  is in standard position. From the description in Lemma 3.2,  $\Omega(E, p; C)$  is a surface ruled by horizontal rays. The rays all attach to  $C$ , which is contained in a plane  $\Pi$ . If  $q \in \Omega$  is any point, let  $q' \in C$  be the point on the same ray as  $q$ .

If  $q = q_1 = (z_1, t_1)$  and  $q_2 = (z_2, t_2)$  are two points in  $\Omega$ , joined by a line segment  $S$ , we define the *slope* of  $S$  to be  $|t_1 - t_2| / |z_1 - z_2|$ . (See Figure 4.) We define the slope of vectors in  $\mathcal{H}$  to be the infinitesimal version of this quantity. Let  $S'$  be the segment joining  $q'_1$  to  $q'_2$ . Note that  $t'_j = t_j$ . If  $q_1$  and  $q_2$  are close together,  $|z'_1 - z'_2| \leq |z_1 - z_2| + O(|z_1 - z_2|^2)$ . Thus, the slope of  $S'$  is less than the slope of  $S$ , up to a second order error. Letting  $q_2 \rightarrow q_1$ , we see that the slope of any vector tangent to  $\Omega$  at  $q$  is less than the maximum slope attained by vectors tangent to  $\Pi$ .

On the other hand,  $\Pi = E_c$ , the contact plane of  $\mathcal{E}$  centered at the center of mass  $c$  of  $C$ . The eccentricity condition implies that  $|\pi_{\mathbf{C}}(c)| < |\pi_{\mathbf{C}}(q)|$  for any point  $q \in \Omega$ . If  $E_q$

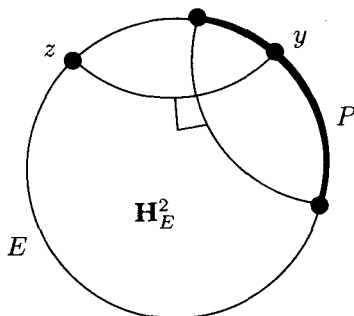


Fig. 5

is the contact plane based at  $q$ , then the maximum slope attained by vectors tangent to  $E_q$  exceeds the maximum slope attained by vectors tangent to  $\Pi = E_c$ . To conclude: The slope of any vector tangent to  $\Omega$  at  $q$  is less than the maximum slope attained by vectors tangent to  $E_q$ . Thus,  $E_q$  cannot be the tangent plane to  $\Omega$  at  $q$ .  $\square$

### 3.5. Loxodromic hybrid spheres

The flag  $(E, p)$  serves as the basis of our definition of the parabolic hybrid cone. Such flags are stabilized by ellipto-parabolic elements. A loxodromic element stabilizes a pair  $(E, P)$ , where  $P \subset E$  is a nontrivial  $\mathbf{C}$ -arc. The inclusion of  $E$  in our notation is redundant, but we wish to highlight the parallels to the parabolic case.

The chain  $E$  bounds a complex slice  $\mathbf{H}_E^2$ . A pair of points  $y \in P$  and  $z \in E - P$  are *harmonic conjugates* if the geodesic  $\gamma_P$  in  $\mathbf{H}_E^2$ , which joins the endpoints of  $P$ , is perpendicular to the geodesic in  $\mathbf{H}_E^2$  which joins  $y$  to  $z$ . (See Figure 5.)

LEMMA 3.5. *Given  $X \in S^3 - E$ , there is a unique  $\mathbf{R}$ -circle  $\gamma(E, P; X)$  which contains  $X$  and which intersects  $E$  in a harmonic pair of points.*

*Proof.* (Compare our proof to the discussion in [G, p. 169].) Let  $\Pi_E$  be orthogonal projection from  $\mathbf{CH}^2$  onto  $\mathbf{H}_E^2$ . The map  $\Pi_E$  extends canonically to  $S^3$ . If  $\gamma \in \mathbf{H}_E^2$  is a geodesic perpendicular to  $\gamma_P$ , then  $\Pi_C^{-1}(\gamma)$  is a spinal sphere whose poles are harmonic conjugates with respect to  $P$ . Such a spinal sphere is the union of  $\mathbf{R}$ -circles, all of which contain both poles. These  $\mathbf{R}$ -circles intersect each other only at the poles. The geodesics perpendicular to  $\gamma_P$  foliate  $\mathbf{H}_E^2$ , so that the spinal spheres, discussed above, foliate  $S^3 - \partial P$ . The point  $X$  lies on one such spinal sphere, and is contained on a unique  $\mathbf{R}$ -circle on this spinal sphere.  $\square$

Let  $\Omega(E, P; X)$  be the portion of  $\gamma(E, P; X)$  which joins  $X$  to  $P$  but which avoids  $E - P$ . Given a subset  $S \subset S^3 - E$  we define the *loxodromic hybrid cone*  $\Omega(E, P; S)$  as in the parabolic case. If  $C$  is a chain which links  $E$ , we define the *loxodromic hybrid sphere*  $\Sigma = \Omega(E, P; C) \cup I_C(\Omega(E, P; C))$ , exactly as in the parabolic case.

### 3.6. Local structure

LEMMA 3.6. *A chain and a spinal sphere intersect in at most two points, unless the spinal sphere contains the chain.*

*Proof.* Normalize so that the spinal sphere is  $(\mathbf{C} \times \{0\}) \cup \infty$ . From here, the lemma is obvious from our description of Heisenberg chains, given in §2.3.  $\square$

Given  $X \in S^3 - P$ , we define the *endpoint map*  $f(X) = \Omega(E, P; X) \cap P$ .

LEMMA 3.7. *Let  $(E, P)$  be as above, and let  $C$  be a chain which links  $E$ . Suppose that  $f|_C$  is not constant. There are two points  $X_1, X_2 \in C$  such that  $f$  is two-to-one on  $C - X_1 - X_2$ , and  $f(C - X_1 - X_2)$  is a  $\mathbf{C}$ -arc bounded by  $f(X_1)$  and  $f(X_2)$ .*

*Proof.* For each  $y \in P$ , the set  $f^{-1}(y)$  is a spinal sphere. By hypothesis,  $C$  is not contained in any such spinal sphere. From this we see that  $f^{-1}(y) \cap C$  consists in at most two points. If we identify  $P$  with some real interval then  $f|_C$  can have at most one maximum point and at most one minimum point. By compactness,  $f$  has at least one maximum point and at least one minimum point. Thus,  $f|_C$  has a unique maximum point  $X_1 \in C$  and a unique minimum point  $X_2 \in C$ . The lemma follows immediately from this.  $\square$

COROLLARY 3.8.  *$\Omega(E, P; C)$  is a piecewise analytic disk.*

*Proof.* Let  $X_1$  and  $X_2$  be the points from the proof of Lemma 3.7. Let  $C_1$  and  $C_2$  be the closed arcs of  $C$  bounded by  $X_1$  and  $X_2$ . We have  $\Omega = \Omega_1 \cup \Omega_2$ . Here  $\Omega_j = \Omega(E, P; C_j)$ . By Lemma 3.7, and the same argument as in Lemma 3.2, the set  $\Omega_j$  is a piecewise analytic disk. The intersection  $\Omega_1 \cap \Omega_2$  is the union of the three analytic arcs  $\Omega(E, P; X_1)$ ,  $\Omega(E, P; X_2)$  and  $f(C_1) = f(C_2)$ . The lemma is clear from this description.  $\square$

*Remark.* Given the picture developed in this section, we see that  $\Sigma(E, P; C)$  is a spinal sphere if and only if  $f|_C$  is constant. The family of loxodromic hybrid spheres contains the family of spinal spheres with codimension 2. In the next section we will see how loxodromic hybrid spheres can be considered as perturbations of parabolic hybrid spheres.

### 3.7. Perturbations

Suppose that  $X$  is a metric space. Given a family of compact subsets  $\{A_\varepsilon\} \subset X$  we write  $A_\varepsilon \rightarrow B$  if and only if  $\delta(A_\varepsilon, B) \rightarrow 0$  as  $\varepsilon \rightarrow 0$ . Here  $\delta(A_\varepsilon, B)$  is the infimal  $r$  such that every point of  $A_\varepsilon$  is within  $r$  of some point of  $B$ , and *vice versa*.

We will take  $X = S^3$  equipped with the round metric, or  $X = \mathcal{H}$  equipped with the Euclidean metric.

Let  $\Sigma_\varepsilon = \Sigma(E_\varepsilon, P_\varepsilon; C_\varepsilon)$  be a family of loxodromic hybrid spheres,  $\Omega_\varepsilon = \Omega(E_\varepsilon, P_\varepsilon; C_\varepsilon)$  be one of the hemispheres of  $\Sigma_\varepsilon$ , and  $\Sigma_0 = \Sigma(E_0, P_0; C_0)$  be a parabolic hybrid sphere. Assume that  $X_\varepsilon \rightarrow X_0$  for  $X = E, P, C$ .

LEMMA 3.9.  $\Sigma_\varepsilon \rightarrow \Sigma_0$ . Furthermore,  $\Sigma_\varepsilon$  is a piecewise analytic embedded sphere, for all sufficiently small  $\varepsilon$ .

*Proof.* We can choose a Heisenberg stereographic projection  $\mathbf{B}_\varepsilon$  so that  $\mathbf{B}_\varepsilon(\mathbf{C}_\varepsilon)$  is the center,  $\mathbf{B}_\varepsilon(P_\varepsilon) \rightarrow \infty$ ,  $\mathbf{B}_\varepsilon(C_\varepsilon) \rightarrow \mathbf{B}_0(C_0)$  and  $\mathbf{B}_\varepsilon \rightarrow \mathbf{B}_0$ , uniformly on compacta. Lemma 3.1 implies that the  $\mathbf{R}$ -circles foliating  $\mathbf{B}_\varepsilon(\Omega_\varepsilon)$  converge, on compacta, to level  $\mathbf{R}$ -circles. In particular, the curvature of these arcs converges uniformly to 0, on compacta. Thus, for any compact  $K \subset \mathcal{H}$ , we have  $K \cap \mathbf{B}_\varepsilon(\Omega_\varepsilon) \rightarrow K \cap \mathbf{B}_0(\Omega_0)$ . Finally,  $\mathbf{B}_\varepsilon^{-1}$  maps small neighborhoods of  $\infty$  to small neighborhoods of  $P_0$ . Hence  $\Sigma_\varepsilon \rightarrow \Sigma_0$ .

In view of Lemma 3.8 and the proof of Lemma 3.2, it suffices to prove that the two hemispheres of  $\Sigma_\varepsilon$  intersect only at the equator. In view of the convergence result  $\Sigma_\varepsilon \rightarrow \Sigma_0$ , it suffices to prove that the two hemispheres intersect only at the equator, in a small neighborhood of the equator. Since  $I_C$  is an involution fixing  $C$ , and rotating each contact plane based at  $C$  by 180 degrees, the  $\mathbf{R}$ -arcs foliating our hemispheres nearly point in opposite directions near  $C$ , as long as  $\varepsilon$  is small.  $\square$

LEMMA 3.10. For any compact set  $K \subset \Omega_0 - P_0$ , there is an open set  $U_K \supset K$  and an  $\varepsilon_K > 0$  such that if  $\varepsilon < \varepsilon_K$  and  $q \in \Sigma_\varepsilon \cap U_K$  then the tangent plane to  $\Sigma_\varepsilon$  at  $q$  is distinct from the contact plane at  $q$ .

*Proof.* The proof of Lemma 3.9 also establishes the following result: Let  $q_\varepsilon \in \Omega_\varepsilon$  be any sequence of points converging to  $q_0 \in \Omega_0 - P_0$ . The tangent plane to  $\Omega_\varepsilon$  at  $q_\varepsilon$  converges to the tangent plane to  $\Omega_0$  at  $q_0$ . From this fact, a sequence of counterexamples to this lemma would lead to a contradiction of Lemma 3.4.  $\square$

#### 4. Parabolic case: discreteness proof

##### 4.1. The parabolic representation

Let  $\varrho: \Gamma \rightarrow \text{Isom}(\mathbf{CH}^2)$  be the parabolic representation. Let  $i_0, i_1, i_2$  be the standard generators of  $\Gamma = \mathbf{Z}/2 * \mathbf{Z}/2 * \mathbf{Z}/2$ . Let  $I_j = \varrho(i_j)$ . The element  $I_j$  is a complex reflection in a chain  $\widehat{C}_j$ . The chains  $\widehat{C}_i$  and  $\widehat{C}_j$  intersect pairwise in a point  $P_{ij}$ . A main feature of  $\varrho$  is that the product of all three generators, taken in any order, is ellipto-parabolic.  $I_i I_j I_k$  fixes a point  $P_j$  and stabilizes a chain  $E_j$ . Since  $I_k I_j I_i$  and  $I_i I_j I_k$  are inverses of each other, they both stabilize the flag  $(E_j, P_j)$ .

$\varrho$  has a very concrete matrix representation. The formulas we give here are special cases of those from [S, §3].

Define

$$\lambda = \frac{1}{16}(5\sqrt{5} + \sqrt{3}i), \quad \mu = \frac{1}{4}(\sqrt{5} + \sqrt{3}i). \quad (14)$$

$\widehat{C}_0, \widehat{C}_1$  and  $\widehat{C}_2$  are, respectively, the chains  $\{z=w\}$ ,  $\{w=\bar{\lambda}\}$  and  $\{z=\lambda\}$ .

Matrix representatives for  $I_0, I_1, I_2$  are, respectively,

$$\begin{bmatrix} 0 & -1 & 0 \\ -1 & 0 & 0 \\ 0 & 0 & -1 \end{bmatrix}, \quad \begin{bmatrix} -1 & 0 & 0 \\ 0 & 3 & -4\bar{\lambda} \\ 0 & 4\lambda & -3 \end{bmatrix}, \quad \begin{bmatrix} 3 & 0 & -4\lambda \\ 0 & -1 & 0 \\ 4\bar{\lambda} & 0 & -3 \end{bmatrix}. \quad (15)$$

The parabolic element  $g = I_1 I_0 I_2$  is represented by

$$g = \begin{bmatrix} 0 & -1 & 0 \\ -\frac{11}{8} - \frac{5}{8}\sqrt{15}i & 0 & \frac{3}{2}\sqrt{3}i \\ -\frac{3}{2}\sqrt{3}i & 0 & -\frac{11}{8} + \frac{5}{8}\sqrt{15}i \end{bmatrix}. \quad (16)$$

Define

$$P_0 = (\mu, \bar{\mu}), \quad Q_0 = (\bar{\lambda}, \lambda). \quad (17)$$

$g$  preserves the pair  $(E_0, P_0)$ , where  $E_0$  is the chain determined by  $P_0$  and  $Q_0$ .

We note that conjugation by the antiholomorphic involution

$$R_0(z, w) = (\bar{w}, \bar{z}) \quad (18)$$

fixes  $I_0$  and interchanges  $I_1$  and  $I_2$ . The chain  $E_0$  is preserved by  $R_0$ . The two fixed points on  $E_0$  are  $P_0$  and  $Q_0$ .

##### 4.2. Canonical projection

There is a canonical Heisenberg stereographic projection  $\mathbf{B}$ , associated to our representation, such that  $\mathbf{B}(E_0)$  is the center of  $\mathcal{H}$  and

$$\mathbf{B}(P_0) = \infty, \quad \mathbf{B}(Q_0) = (0, 0), \quad \mathbf{B}(P_{12}) = (1, 0).$$

We write  $\mathbf{B}=\pi\circ\beta$ , as in equation (5), and  $\beta=\Theta\circ M\circ\Theta^{-1}$ , where  $\Theta$  is as in equation (3) and  $M$  is some matrix, not necessarily in  $PU(2,1)$ . Scaling  $M$  has no effect on the resulting Heisenberg stereographic projection.

Here is how we derive  $M$ . The points  $P_{12}, P_0, Q_0$  all lie on the  $\mathbf{R}$ -circle fixed by  $R_0$ . We can choose lifts  $\tilde{P}_0, \tilde{Q}_0$  and  $\tilde{P}_{12}$ , and a polar vector  $E^*$ , such that

$$\langle \tilde{P}_0, \tilde{Q}_0 \rangle = \langle \tilde{Q}_0, \tilde{P}_{12} \rangle = \langle \tilde{P}_{12}, \tilde{P}_0 \rangle = \langle E^*, \tilde{P}_{12} \rangle = -1.$$

(This follows from the vanishing of the *angular invariant* of  $P_0, Q_0, P_{12}$ . See [G] for details.) We define

$$\hat{M}(X) = (\langle \tilde{X}, E^* \rangle, \langle \tilde{X}, \tilde{Q}_0 \rangle, \langle \tilde{X}, \tilde{P}_0 \rangle). \quad (19)$$

Up to scale, the matrix representing  $\hat{M}$  is

$$M = \begin{bmatrix} -6\sqrt{5} + 2\sqrt{3}i & -6\sqrt{5} - 2\sqrt{3}i & 18 \\ 10\sqrt{5} + 2\sqrt{3}i & 10\sqrt{5} - 2\sqrt{3}i & -32 \\ 3\sqrt{5} - 3\sqrt{3}i & 3\sqrt{5} + 3\sqrt{3}i & -12 \end{bmatrix}. \quad (20)$$

### 4.3. Proof modulo disjointness

We now associate a parabolic hybrid sphere  $\Sigma_j$  to each generator  $I_j$  of the ideal triangle group. We will describe  $\Sigma_1$ . The other two are obtained by cyclically permuting the indices. The equator of  $\Sigma_1$  is  $\hat{C}_1$ , the chain fixed by  $I_1$ . One of the spines of  $\Sigma_1$  is the pair  $(E_0, P_0)$  stabilized by  $I_1 I_0 I_2$ . The other spine is the pair  $(E_2, P_2)$  stabilized by  $I_1 I_2 I_0$ .

Let  $\xi$  be cylindrical projection, defined in §2.4. Figure 6 shows the images  $\xi(\mathbf{B}(\Sigma_1))$  and  $\xi(\mathbf{B}(\Sigma_2))$ . Here  $\Xi$  is identified with  $[0, 2\pi] \times \mathbf{R}$ , with vertical sides identified, and the images have been scaled so as to fit nicely in a square. It appears that one of these sets intersects the other in a single point. The inverse image of this point is an  $\mathbf{R}$ -arc. The justification for this picture is the proof, following this section, of the Disjointness Lemma.

LEMMA 4.1 (Disjointness Lemma).  $\Sigma_1 \cap \Sigma_2 = \Omega(E_0, P_0; P_{12})$ .

COROLLARY 4.2. *The parabolic representation  $\rho$  is discrete and faithful.*

*Proof.* By cyclically permuting the indices, we see that  $\Sigma_i$  and  $\Sigma_j$  intersect in an arc, for each pair of indices  $i \neq j$ . Each sphere bounds two open balls. Since the arc does not disconnect either sphere, one of the two open balls in  $S^3$  bounded by  $\Sigma_1$  is disjoint from one of the two open balls in  $S^3$  bounded by  $\Sigma_2$ . It follows from the threefold symmetry of the picture that there are open balls  $B_j$ , which are bounded by  $\Sigma_j$ , such that  $B_0, B_1, B_2$



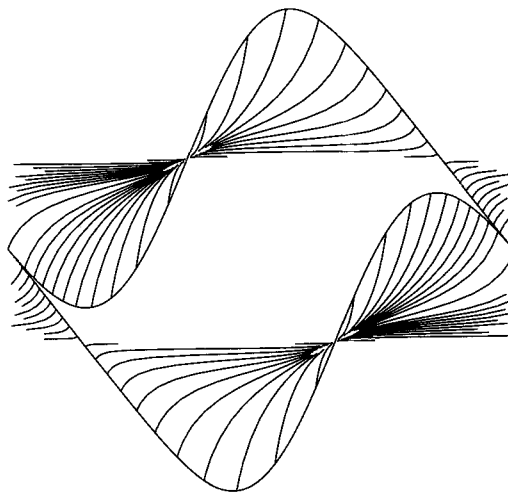


Fig. 6

are pairwise disjoint. The element  $I_j$  stabilizes  $\Sigma_j$  and maps the complement of  $\bar{B}_j$  into  $B_j$ . Here  $\bar{B}_j$  is the closure of  $B_j$ .

We end our proof with an argument reminiscent of the Ping-Pong Lemma. Let  $w$  be any reduced word in  $\{i_0, i_1, i_2\}$ . We have  $w = i_{a_n} \dots i_{a_1}$ , where  $a_j \in \{1, 2, 3\}$  and  $a_i \neq a_{i+1}$  for any index  $i$ . We have  $w = a_n w'$ , where  $w' = i_{a_{n-1}} \dots i_{a_1}$ . By induction,  $\varrho(w')$  maps the complement of  $\bar{B}_{a_1}$  into  $B_{a_{n-1}}$ . Since  $a_n \neq a_{n-1}$ , the disjointness above says that  $\varrho(w)$  maps the complement of  $\bar{B}_{a_1}$  into the interior of  $B_{a_n}$ . As usual, this is enough to conclude that  $\varrho$  is discrete and faithful.  $\square$

#### 4.4. Disjointness proof modulo two lemmas

We will write  $\mathbf{B}(\Sigma_j) = \Omega_j \cap \Omega'_j$ , where  $\Omega'_j$  is in standard position and  $\Omega_j = I_{C_j}(\Omega'_j)$ . Here  $C_j = \mathbf{B}(\hat{C}_j)$ . Let  $c_j$  be the center of mass of  $C_j$ . For  $j=1, 2$ , define

$$S_j = \xi(C_j), \quad H_j = \mathbf{R}/2\pi\mathbf{Z} \times \pi_{\mathbf{R}}(c_j).$$

Let  $R_j \subset \Xi$  be the region bounded by  $S_j$  and  $H_j$ . (See Figure 7.)

LEMMA 4.3.  $R_1 \cap R_2$  is a single point, disjoint from  $H_1 \cup H_2$ .

LEMMA 4.4.  $\xi(\Omega_j) \subset R_j$  and  $\xi(\Omega_j - C_j) \cap S_j \subset H_j$ .

Let us now deduce the Disjointness Lemma.  $\xi$  maps level  $\mathbf{R}$ -circles to single points. For this reason,  $\xi(\Omega'_j) \subset \xi(C_j)$ . Lemma 4.3 therefore says that  $\Omega'_1 \cap \Omega'_2$  is a single  $\mathbf{R}$ -arc.

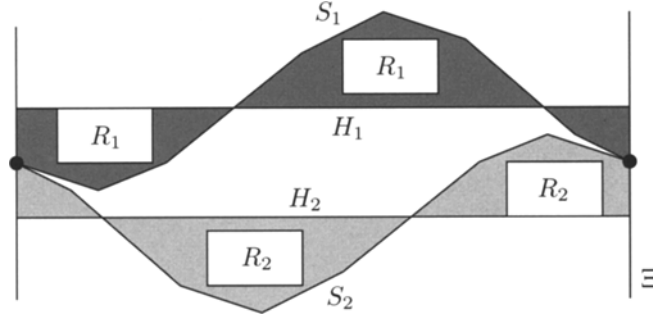


Fig. 7

This  $\mathbf{R}$ -arc must be contained in a level  $\mathbf{R}$ -circle, must reach  $\infty$ , and must have  $(1, 0)$  as its finite endpoint. Hence  $\Omega'_1 \cap \Omega'_2 = [1, \infty]$ . We have

$$\xi(\Omega_1 - C_1) \subset (R_1 - S_1) \cup H_1 = X, \quad \xi(\Omega'_2) \subset S_2 = Y.$$

$X \cap Y = \emptyset$ , by Lemma 4.3. Since  $\xi$  is defined on all of  $\Omega_1 - C_1$ , and  $\infty \notin \Omega_1$ , we have  $(\Omega_1 - C_1) \cap C_2 = \emptyset$ . Similarly,  $(\Omega_2 - C_2) \cap C_1 = \emptyset$ . Lemma 4.4 immediately implies that  $\xi(\Omega_1 - C_1) \cap \xi(\Omega_2 - C_2) = \emptyset$ , and hence  $(\Omega_1 - C_1) \cap (\Omega_2 - C_2) = \emptyset$ . All in all, we find that  $\mathbf{B}(\Sigma_1) \cap \mathbf{B}(\Sigma_2) = [1, \infty]$ . By construction,  $[1, \infty] = \mathbf{B}(\Omega(E_0, P_0; P_{12}))$ . This establishes the Disjointness Lemma.

#### 4.5. Proof of Lemma 4.3

Using equation (20) and the equations in §4.1 we compute that

$$c_1 = \mathbf{B} \circ I_{C_1} \circ \mathbf{B}^{-1}(\infty) = \left( -\frac{1}{4} + \frac{\sqrt{5}}{4\sqrt{3}}i, \frac{\sqrt{15}}{4} \right). \quad (21)$$

Using  $\mathbf{B}(P_{12}) = (1, 0)$  and equation (21) we see that

$$\varrho(\pi_{\mathbf{C}}(C_1)) = \sqrt{5/3}, \quad |\pi_{\mathbf{C}}(c_1)| = \sqrt{1/6}. \quad (22)$$

The map  $(z, t) \rightarrow (\bar{z}, -t)$  interchanges  $C_1$  and  $C_2$ , as well as  $\Sigma_1$  and  $\Sigma_2$ . Therefore, all information about  $\Sigma_2$  can be obtained from the formulas above.

$S_i$  and  $H_j$  are graphs of  $2\pi$ -periodic functions  $s_i$  and  $h_j$ . Equation (21) gives

$$h_1(\theta) \equiv \frac{1}{4}\sqrt{15}, \quad h_2(\theta) \equiv -\frac{1}{4}\sqrt{15}. \quad (23)$$

Referring to Lemma 2.1, as applied to  $C_1$ , we have

$$\begin{aligned} \theta_0 \in \left( \frac{1}{2}\pi, \pi \right), \quad \tan(\theta_0) = -\sqrt{5/3}, \\ A = \frac{1}{3}, \quad B = \frac{1}{4}\sqrt{15} = g(\theta_0), \quad \varrho = \sqrt{5/3}, \quad E = 9. \end{aligned} \quad (24)$$

Hence,

$$s_1(\theta) = g(\theta - \theta_0) + g(\theta_0), \quad s_2(-\theta) = -s_1(\theta), \quad (25)$$

$$3g(\theta) = \sin(\theta)(\cos(\theta) + \sqrt{\cos^2(\theta) + 9}). \quad (26)$$

To prove Lemma 4.3 it suffices to prove that

- (1)  $s_1(\theta) > h_2(\theta)$  for all  $\theta$ ,
- (2)  $s_2(\theta) < h_1(\theta)$  for all  $\theta$ ,
- (3)  $s_1(\theta) = s_2(\theta)$  if and only if  $\theta = 2\pi k$  for  $k \in \mathbf{Z}$ .

We compute

$$3g'(\theta) = 2\cos^2(\theta) - 1 + \frac{\cos(\theta)(2\cos^2(\theta) + 8)}{\sqrt{\cos^2(\theta) + 9}}.$$

From this it follows that  $g'(\theta) = 0$  if and only if  $\cos(\theta) = 1/\sqrt{11}$ . Plugging this into  $g$ , we get  $|g(\theta)| \leq \frac{1}{3}\sqrt{10}$ . In particular,

$$s_1(\theta) > -\frac{1}{3}\sqrt{10} + g(\theta_0) = -\frac{1}{3}\sqrt{10} + \frac{1}{4}\sqrt{15} > -\frac{1}{4}\sqrt{15} = h_2(\theta).$$

This is statement (1). Statement (2) follows from symmetry.

For statement (3), note first that  $s_1(0) = s_2(0) = 0$ . By symmetry, and periodicity, it suffices to prove that  $s_1(\theta) > s_2(\theta)$  for  $\theta \in [\pi, 2\pi)$ . Define  $\theta_1 = \theta_0 - \pi \in (-\frac{1}{2}\pi, 0)$ . Note that  $|\theta - \theta_0| < |\theta_1|$  implies  $\theta \in (\pi, 2\pi)$ . We compute that  $g''(\theta)$  is a positive multiple of  $A_1 A_2 A_3 A_4$ , where

$$A_1 = -\sin(\theta), \quad A_2 = (9 + \cos^2(\theta))^{-3/2}, \quad A_3 = \cos(\theta) + \sqrt{9 + \cos^2(\theta)},$$

$$A_4 = 10\cos(\theta) + (4 + \cos^2(\theta))(\cos(\theta) + \sqrt{9 + \cos^2(\theta)}).$$

Note that  $A_j(\theta) > 0$  for  $j = 1, 2, 3$  and  $\theta \in (\pi, 2\pi)$ . If  $A_4(\theta) = 0$ , then

$$\cos(\theta) = -\frac{\sqrt{30\sqrt{5} - 54}}{\sqrt{11}}.$$

From this, and from  $A_4(-\theta_0) > 0$ , we get  $A_4(\theta) > 0$  for  $|\theta + \theta_0| < |\theta_1|$ . Hence,

$$g''(\theta) > 0, \quad |\theta + \theta_0| < |\theta_1|. \quad (27)$$

By symmetry,

$$s_1'(0) = s_2'(0), \quad s_1''(\theta) = -s_2''(\theta). \quad (28)$$

From equations (27) and (28), we get

$$s_1''(\theta) > 0, \quad s_2''(\theta) < 0, \quad \theta \in (\theta_1, -\theta_1). \quad (29)$$

By equations (28) and (29), integration, and periodicity,

$$s_1(\theta) > s_2(\theta), \quad \theta \in [\theta_1 + 2\pi, 2\pi). \quad (30)$$

Since  $g(\theta) > 0$  for  $\theta \in (0, \pi)$ , we have

$$s_1(\theta) > g(\theta_0) = h_1(\theta) > s_2(\theta), \quad \theta \in (\theta_0, \theta_1 + 2\pi] \supset [\pi, \theta_1 + 2\pi]. \quad (31)$$

Statement (3) follows immediately from equations (30) and (31).

#### 4.6. Proof of Lemma 4.4

We will deduce Lemma 4.4 from a more general result, which might have other uses. Say that a hybrid hemisphere  $\Omega$  is in *inverted position* if  $I_C(\Omega)$  is in standard position. Here  $C$  is the equator of  $\Omega$ , and  $I_C$  is complex reflection in  $C$ . Let  $c$  be the center of mass of  $C$ . Let  $R \subset \Xi$  be the region bounded by

$$S = \xi(C), \quad H = \mathbf{R}/2\pi\mathbf{Z} \times \pi_{\mathbf{R}}(c).$$

Lemma 4.4 is an instance of

LEMMA 4.5 (Dollar Sign). *Let  $\Omega$  be a tame hybrid sphere with positive eccentricity. If  $\Omega$  is in inverted position then  $\xi(\Omega) \subset R$  and  $\xi(\Omega - C) \cap S \subset H$ .*

Normalizing by a map from equation (9), we can arrange that  $c = (t, 0)$ , where  $t > 0$ . Thus,  $S \cap H = (0, 0)$ . Let  $L = \mathbf{R} \times \{0\}$ . Note that  $L \cup \infty$  is a Heisenberg  $\mathbf{R}$ -circle which intersects  $C$  in two points. Define the open topological disks

$$\Omega_+ = \{(z, t) \in \Omega \mid \text{Im}(z) > 0\} - C \quad \text{and} \quad \Omega_- = \{(z, t) \in \Omega \mid \text{Im}(z) < 0\} - C.$$

We will show that the fibers of  $\xi$  are transverse to  $\Omega_{\pm}$ . (It suffices to consider  $\Omega_+$ , by symmetry.) By the Open Mapping Theorem,  $\xi(\Omega_{\pm}) \subset R - \partial R$ . The Dollar Sign Lemma follows from this, and from the straightforward items

- (1)  $\Omega - \Omega_+ - \Omega_- \subset C \cup L$ ,
- (2)  $\bar{\Omega}_{\pm} - \Omega_{\pm} \subset C \cup L$ ,
- (3)  $\xi(C \cup L) \subset \partial R$ ,
- (4)  $\xi(C - L) \subset S - H$ .

$\Omega$  is foliated by  $\mathbf{R}$ -arcs, one of which is  $L \cap \Omega$ . Hence  $\Omega_+$  is also foliated by  $\mathbf{R}$ -arcs. Say that an *inward radial* is a curve of the form  $\pi_C(\alpha)$ , where  $\alpha$  is one of the foliating  $\mathbf{R}$ -arcs of  $\Omega_+$ . The inward radials are line segments or arcs of lemniscates.

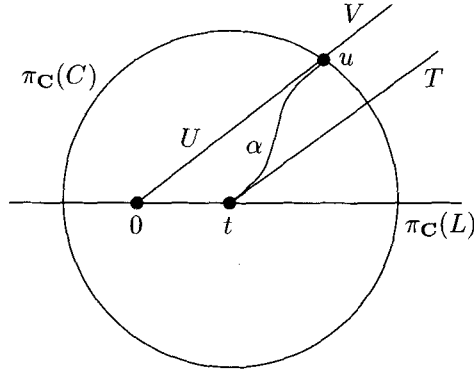


Fig. 8

LEMMA 4.6. *If a fiber of  $\xi \circ \mathbf{B}$  is tangent to  $\Omega_+$  then some ray through the origin is tangent to some inward radial  $\alpha$ , at an interior point  $y \in \alpha$ .*

*Proof.* The fibers of  $\xi$  have the form  $\varrho_s = \varrho \times \{s\}$ , where  $\varrho$  is a ray through the origin in  $\mathbf{C}$ . If a fiber of  $\xi$  is tangent to  $\Omega_+$  then there is some  $s \in \mathbf{R}$ , some ray  $\varrho$ , and some  $x \in \Omega_+$ , such that  $\varrho_s$  is tangent to  $\Omega_+$  at  $x$ . Let  $T_x$  be the tangent plane to  $\Omega_+$  at  $x$ . Let  $E_x$  be the contact plane. Equation (22) says that  $\Sigma$  has eccentricity  $\sqrt{1/10}$ , and hence is tame. By Lemma 3.4, we have  $E_x \neq T_x$ . Let  $\alpha_x$  be the foliating  $\mathbf{R}$ -arc through  $x$ . Both  $\varrho_s$  and  $\alpha_x$  are CR-horizontal and tangent to  $\Omega_+$ . Hence,  $\varrho_s$  and  $\alpha_x$  are tangent to two unequal planes, and hence to each other. Projecting, we see that  $\varrho$  and  $\pi_{\mathbf{C}}(\alpha_x)$  are tangent to each other at  $\pi_{\mathbf{C}}(x)$ , which is in the interior of  $\alpha = \pi_{\mathbf{C}}(\alpha_x)$ .  $\square$

Say that an arc of a lemniscate is *symmetric* if it contains the double point and has 180 degree rotational symmetry. We say that such an arc is *small* (resp. *medium*) if its arc length is less than (resp. equal to) half that of the lemniscate.

LEMMA 4.7. *The inward radial  $\alpha$  is a small symmetric arc.*

*Proof.* Recall that  $\alpha = \pi_{\mathbf{C}}(\alpha_x)$ . One endpoint of  $\alpha$  is  $t$ , and the other is some  $u \in \pi_{\mathbf{C}}(C)$ . Let  $T$  and  $U$  be the tangent lines to  $\alpha$  at  $t$  and  $u$  respectively. (See Figure 8.)

Let  $\alpha'_x = I_C(\alpha_x)$ . Note that  $\alpha'_x$  is an arc of a level  $\mathbf{R}$ -circle, since  $I_C(\Omega)$  is in standard position. Since  $I_C$  interchanges  $(t, 0)$  and  $\infty$  it follows from symmetry that the line  $V$  containing  $\pi_{\mathbf{C}}(\alpha'_x)$  is parallel to  $T$ . The differential map  $dI_C$  acts as a 180 degree rotation of the contact planes which are based at points of  $C$ , so that  $U = V$ . In short,  $T$  and  $U$  are parallel. Since  $0, t$  and  $u$  are not collinear,  $\alpha$  is not a line segment.

Let  $S$  be the space of arcs of lemniscates which have tangent lines parallel at the endpoints, given the topology from the top of §3.7—that is, the *Hausdorff topology*.  $S$  has several components, one of which is  $S_0$ , the subset of symmetric arcs.  $S_0$  is the

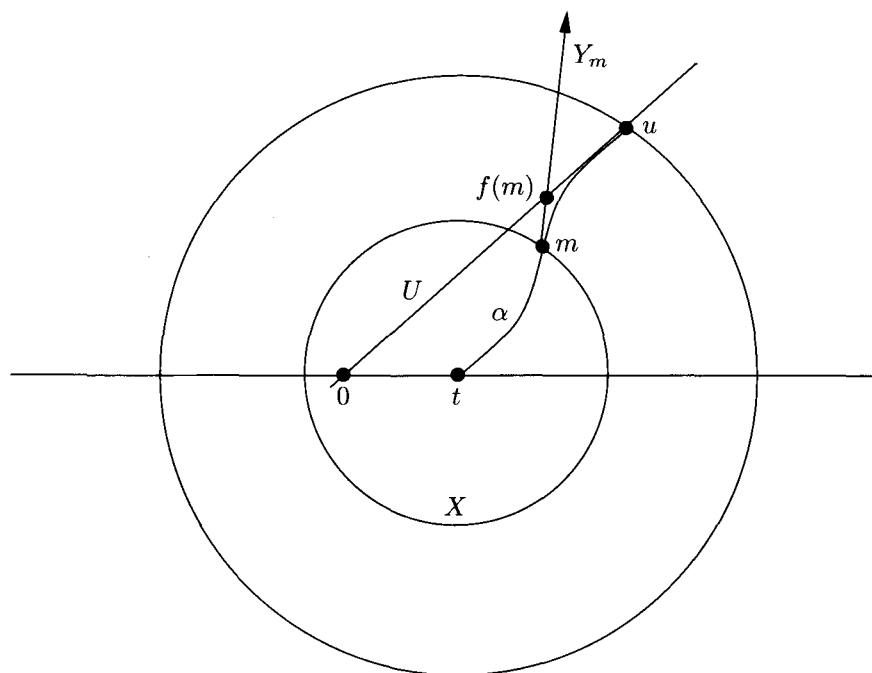


Fig. 9

only component which has elements which converge to a line segment.  $\alpha$  is nearly a line segment for choices of  $\alpha$  near  $L$ . Hence,  $\alpha \in S_0$  for all choices of  $\alpha$ . Also,  $U$  is never tangent to  $\pi_{\mathbf{C}}(C)$ , so that  $\alpha$  is not a medium symmetric arc. Since some choices of  $\alpha$  are small symmetric arcs, and no choice is a medium symmetric arc, all choices are small symmetric arcs.  $\square$

Figure 9 shows the construction to follow. Let  $m \in \alpha$  be the midpoint. Let  $X$  be the disk centered at  $t$  such that  $m \in \partial X$ . For  $y \in \alpha$  an interior point, let  $Y_y$  be the ray tangent to  $\alpha$ , at  $y$ , oriented away from  $t$ . (This ray is shown for  $y = m$ .) Since  $\alpha$  is a small symmetric arc,  $\alpha$  is always transverse to  $\partial X$ , and pointing outward, when oriented towards  $\pi_{\mathbf{C}}(C)$ . That is,  $Y_m \cap X \subset \partial X$ . Since  $\Omega$  is tame, and  $\partial X$  has half the diameter of  $\pi_{\mathbf{C}}(C)$ , we have  $0 \in X - \partial X$ . In particular,  $0 \notin Y_m$ .

$Y_y$  is never parallel to  $U$ , because  $\alpha$  is a small symmetric arc. If  $Y_y \cap U = \emptyset$  for some choice of  $y$ , then  $Y_y \cap U = \emptyset$  for all choices. For  $y$  close to  $u$  we obviously have  $Y_y \cap U \neq \emptyset$ . Hence,  $Y_y \cap U \neq \emptyset$  for all interior points  $y$ . We define

$$f(y) = \text{Im}(Y_y \cap U).$$

If we can show that  $f(y) > 0$  we will know that the line tangent to  $\alpha$  at  $y$  does not contain the origin, as desired.

$f$  is monotone on each convex half of  $\alpha$ , and attains its minimum at  $m$ . If  $f(m) > 0$  then  $f(y) > 0$  for all interior  $y$ . Since  $0 \notin Y_m$ , we have  $f(m) \neq 0$ . There are some choices of  $\alpha$  for which  $f(m) > 0$ . Since we have shown that  $f(m) = 0$  is impossible for any choice, we conclude that, always,  $f(m) > 0$ .

## 5. The action of parabolics

### 5.1. Overview

Say that a sequence of subsets  $\{X_n\} \subset S^3$  *shrinks to a point*  $x \in S^3$  if each open neighborhood  $U$  of  $x$  contains  $X_n$ , once  $n$  is greater than some integer  $N_U$ . The purpose of this chapter is to prove Lemmas 5.1 and 5.2 below. The notation is from §4.

LEMMA 5.1. *The sequence  $\{(I_1 I_0 I_2)^n(\Sigma_1) \mid n \in \mathbf{N}\}$  shrinks to the point  $P_0$ .*

*Proof.* Let  $g = I_1 I_0 I_2$ . Recall that  $g$  stabilizes the flag  $(E_0, P_0)$ , which is a spine of  $\Sigma_1$ . We normalize by the Heisenberg stereographic projection  $\mathbf{B}$ , from §4, so that  $\mathbf{B}(E_0)$  is the center and  $\mathbf{B}(P_0) = \infty$ . Note that  $\mathbf{B}(\Sigma_1) - \infty$  is contained in an infinite slab of the form  $S_K = \{(z, t) \mid |t| < K\}$ . Here  $K$  is some constant. Let  $\gamma = \mathbf{B} \circ g \circ \mathbf{B}^{-1}$ . The element  $g$  is ellipto-parabolic, so that  $\gamma(z, t) = (uz, t + t_0)$ . Here  $t_0$  is some nonzero real number. Note that  $\{\gamma^n(S_K)\}$  exits every compact subset of  $\mathcal{H}$ . The same is therefore true for  $\{\gamma^n(\mathbf{B}(\Sigma_1))\}$ . Pulling back by  $\mathbf{B}$  gives us our result.  $\square$

LEMMA 5.2. *The sequence  $\{(I_1 I_2)^n(\Sigma_1) \mid n \in \mathbf{N}\}$  shrinks to the point  $P_{12}$ .*

*Proof.* Let  $\mathbf{P}$  be a Heisenberg stereographic projection so that  $\mathbf{P}(P_{12}) = \infty$ . Let  $h = \mathbf{P} \circ I_1 I_2 \circ \mathbf{P}^{-1}$ . Let  $\Psi = \mathbf{P}(\Sigma_1)$ . It suffices to prove that  $\{h^n(\Psi)\}$  exits every compact subset of  $\mathcal{H}$ . If this is false, then there is a hemisphere  $\Upsilon$  of  $\Psi$ , points  $p_j = (z_j, t_j) \in \Upsilon$ , and an increasing sequence  $\{n_j\}$  such that  $p_j \rightarrow \infty$  and  $\{h^{n_j}(p_j)\}$  is precompact in  $\mathcal{H}$ .

We may write  $h = h_1 h_2$ , where  $h_j = \mathbf{P} \circ I_j \circ \mathbf{P}^{-1}$ . Since  $\mathbf{P}(\widehat{C}_j)$  is a vertical chain,  $h_j$  covers order-2 rotation about the point  $\pi_{\mathbf{C}}(C_j)$ . Hence,  $h$  covers translation along the line  $M \subset \mathbf{C}$  which joins these two points. Suitably choosing  $\mathbf{P}$ , we can assume that  $M$  is the real axis. In this case  $h$  has the form given in equation (8), with  $z_0 \in \mathbf{R}$ . From this we see that  $|\operatorname{Im}(z_j)|$  is uniformly bounded and  $|t_j| < C_1 |z_j| + C_1$  for some constant  $C_1$ .

The remainder of this chapter is devoted to establishing the lower bound  $|t_j| > C_7 |z_j|^2 - C_7$  for some constant  $C_7$ . For  $j$  sufficiently large, the two bounds contradict each other.  $\square$

### 5.2. Positions of lines

Recall that  $\widehat{C}_1$  is the equator of  $\Sigma_1$ . This hybrid sphere has  $(E_0, P_0)$  as one of its spines.

LEMMA 5.3. *Let  $\Omega_1$  be the hemisphere of  $\Sigma_1$  which has  $(E_0, P_0)$  as a spine. Let  $\gamma$  be the  $\mathbf{R}$ -circle containing  $\Omega(E_0, P_0; P_{12})$ . Then  $\gamma \cap \widehat{C}_1 = P_{12}$ .*

*Proof.* We already know that  $P_{12} \in \gamma \cap \widehat{C}_1$ . We just have to show that  $\gamma$  does not intersect  $\widehat{C}_1$  twice. A horizontal line intersects a Heisenberg chain twice if and only if the line contains the center of mass of the chain. Let  $\mathbf{B}$  be the Heisenberg stereographic projection from §4.1. Recall that  $\mathbf{B}(\gamma) = \mathbf{R} \times \{0\}$  and that  $C_1 = \mathbf{B}(\widehat{C}_1)$  is an elliptical Heisenberg chain whose center of mass is not contained in  $\mathbf{R} \times \{0\}$ . From this we see that  $C_1$  does not intersect  $\mathbf{B}(\gamma)$  twice. Pulling back by  $\mathbf{B}$  we get our result.  $\square$

Let  $\alpha$  be the foliating  $\mathbf{R}$ -arc of  $\Upsilon$  which connects  $p = \mathbf{P}(P_{12})$  to  $\infty$ . Let  $\widehat{\alpha}$  be the straight Heisenberg  $\mathbf{R}$ -circle which contains  $\alpha$ . Let  $L = \pi_{\mathbf{C}}(\alpha)$ . Let  $\Upsilon'$  be the other hemisphere of  $\Psi$ . For each object  $X$  just defined, let  $X'$  be the corresponding object on  $\Upsilon'$ .

COROLLARY 5.4.  *$\widehat{\alpha}$  and  $\widehat{\alpha}'$  do not intersect the equator  $C = \mathbf{P}(\widehat{C}_1)$  of  $\Psi$  in  $\mathcal{H}$ . Thus the lines  $L$  and  $L'$  are distinct and parallel.*

*Proof.* The complex reflection  $I_C$  fixes  $C$ .  $I_C$  interchanges  $\widehat{\alpha}$  and  $\widehat{\alpha}'$ . Hence, the corollary is true for  $\widehat{\alpha}$  if and only if it is true for  $\widehat{\alpha}'$ . For  $\widehat{\alpha}''$  one of  $\widehat{\alpha}, \widehat{\alpha}'$  we have  $\widehat{\alpha}'' = \mathbf{P}(\gamma)$ . Pulling back by  $\mathbf{P}$ , the previous result tells us that  $\widehat{\alpha}'' \cap C = \infty$ . Note that  $I_C$  covers order-2 rotation which swaps  $L$  and  $L'$ . This fixed point is contained on neither line. Hence,  $L$  and  $L'$  are distinct and parallel.  $\square$

LEMMA 5.5.  *$L$  and  $M$  are perpendicular.*

*Proof.* In the notation of the previous lemma, it suffices to prove that  $L'' = \pi_{\mathbf{C}}(\widehat{\alpha}'')$  and  $M$  are perpendicular.  $R_0$  swaps  $\widehat{C}_1$  and  $\widehat{C}_2$ , and preserves  $\widehat{C}_0$ . Hence,  $R_0$  swaps  $\Sigma_1$  and  $\Sigma_2$ , and fixes  $\gamma$ . Let  $R = \mathbf{P} \circ R_0 \circ \mathbf{P}^{-1}$ . Note that  $R$  is an involution which fixes both  $\widehat{\alpha}''$  and  $\infty$ . Also,  $R$  swaps the vertical chains  $C_1 = \mathbf{P}(\widehat{C}_1)$  and  $C_2 = \mathbf{P}(\widehat{C}_2)$ . Hence,  $R$  covers reflection in  $L''$ , and this reflection swaps the points  $\pi_{\mathbf{C}}(C_1)$  and  $\pi_{\mathbf{C}}(C_2)$ . This is only possible if  $L''$  and  $M$  are perpendicular.  $\square$

### 5.3. The lower bound

Before we give our proof, let us summarize what we know so far.  $\Upsilon$  is a hemisphere of  $\Psi = \mathbf{P}(\Sigma_1)$ . The equator  $C = \mathbf{P}(\widehat{C}_1)$  of  $\Upsilon$  is a vertical chain which projects to a point under  $\pi_{\mathbf{C}}$ . The pole of  $\Upsilon$  is the point  $p = \mathbf{P}(P_0)$ . The  $\mathbf{R}$ -arc foliating  $\Upsilon$ , which connects



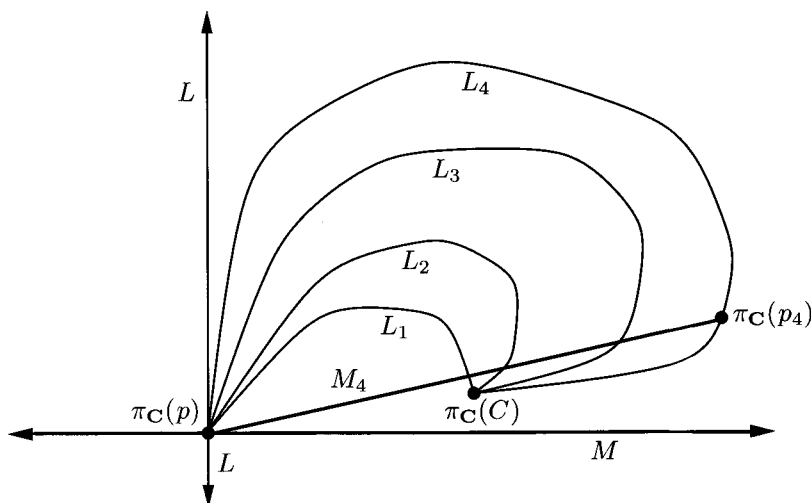


Fig. 10

$\infty$  to  $p$ , projects to a ray parallel to the imaginary axis. The element  $h$  covers translation along the real axis. The points  $p_1, p_2, \dots$  are points on  $\Upsilon$  which converge to  $\infty$ , and are such that  $h^{n_j}(p_j)$  is contained in a fixed compact subset of  $\mathcal{H}$ .

Now for the proof. Let  $\alpha_j$  be the foliating  $\mathbf{R}$ -arc of  $\Upsilon$  which contains  $p_j$ . Let  $L_n = \pi_{\mathbf{C}}(\alpha_j)$ . Let  $P$  be the vertical chain  $\pi_{\mathbf{C}}^{-1}(p)$ . There is a unique straight  $\mathbf{R}$ -arc  $\beta_j$  which connects a point  $p'_j \in P$  to  $p_j$ . Let  $M_j = \pi_{\mathbf{C}}(\beta_j)$ . Since  $|z_n| \rightarrow \infty$  and  $|\text{Im}(z_n)|$  is bounded,  $M_n$  converges to  $M$ . (See Figure 10.)

LEMMA 5.6. *There are similarities  $T_n: \mathbf{C} \rightarrow \mathbf{C}$  such that  $T_n(L_n)$  converges to one lobe of the unit lemniscate, as  $n \rightarrow \infty$ . The expansion constant of  $T_n^{-1}$  tends to  $\infty$  with  $n$ .*

*Proof.* First of all, the unit tangent vector to  $L_n$  at  $\pi_{\mathbf{C}}(p)$  converges to a unit vector tangent to  $L$ . Call this Fact 1.

We claim that  $L_n$  is an arc of a lemniscate  $\hat{L}_n$ , for  $n$  sufficiently large. If this is false, then  $L_n$  is a ray.  $L_n$  contains the point  $\pi_{\mathbf{C}}(C)$ , which is not contained in  $L$ . Hence, there is a uniformly positive bound on the angle between  $L$  and  $L_n$ , contradicting Fact 1.

We choose a similarity  $T_n$  such that  $T_n(\hat{L}_n)$  is the unit lemniscate. The diameter of  $L_n$  tends to  $\infty$  with  $n$ , because  $\pi_{\mathbf{C}}(\alpha)$  is noncompact. Thus, the expansion constant of  $T_n^{-1}$  tends to  $\infty$ . The endpoints of  $L_n$  are  $x = \pi_{\mathbf{C}}(C)$  and  $y = \pi_{\mathbf{C}}(p)$ , points which are independent of  $n$ . Since the expansion constant of  $T_n$  tends to 0, the two points  $T_n(x)$  and  $T_n(y)$  converge to the same point, which must be the double point of the unit lemniscate—that is, the origin.

Thus, either  $T_n(L_n)$  converges to one lobe of the unit lemniscate, or to the entire lemniscate. In the second case,  $\hat{L}_n - L_n$  is contained in a single compact subset  $K$  of  $\mathbf{C}$ ,

independent of  $n$ . By compactness, there is a uniform upper bound to the length of  $\widehat{\alpha}_n - \alpha_n$ , and hence to the distance between the endpoints of  $\alpha_n$ . Here  $\widehat{\alpha}_n$  is the  $\mathbf{R}$ -circle containing  $\alpha_n$ . This contradicts the fact that one endpoint of  $\alpha_n$  tends to  $\infty$ , and the other one is  $p \in \mathcal{H}$ .  $\square$

Let  $C_1, C_2, \dots$  denote constants. Since  $\beta_j$  is contained in a contact plane parallel to the one based at  $p$ , we see that  $|t'_j - t_j| < C_1|z_j| + C_1$ . Note that  $L_j$  has diameter at least  $C_2|z_j| - C_2$ . By Lemma 5.6, and from the convergence of  $M_j$  to  $M$ , we see that  $L_j \cup M_j$  bounds a region with signed area at least  $C_4|z_j|^2 - C_4$ . As we discussed in §2.3, the CR-horizontal lift  $\alpha_j \cup \beta_j$  has monodromy at least  $C_5|z_j|^2 - C_5$ . That is,  $|t'_j| > C_6|z_j|^2 - C_6$ . The triangle inequality now says that  $|t_j| > C_7|z_j|^2 - C_7$ .

This completes our proof of Lemma 5.2.  $\square$

## 6. Domain of discontinuity and limit set

### 6.1. Main result

We know from §4 that the parabolic representation  $\varrho$  is a discrete embedding. Let  $\Lambda \subset S^3$  be the limit set of  $\varrho(\Gamma)$ , and let  $\Delta = S^3 - \Lambda$  be the domain of discontinuity. In this chapter we will describe  $\Lambda$  and  $\Delta$ .

Let  $\Sigma_0, \Sigma_1, \Sigma_2$  be the hybrid spheres constructed in §4. These spheres bound the disjoint open balls  $B_0, B_1, B_2$ , used in the proof of Corollary 4.2. Recall that  $P_{ij}$  is the fixed point of  $I_i I_j$ . Let  $P_k$  be the fixed point of  $I_{k-1} I_k I_{k+1}$ . Here indices are taken mod 3. Note that  $P_{ij}, P_k \subset \Sigma_0 \cup \Sigma_2 \cup \Sigma_2$ . Define

$$F = S^3 - \bigcup B_i - \bigcup P_{ij} - \bigcup P_k. \quad (32)$$

$F$  is obtained by deleting six points from the closed set  $S^3 - \bigcup B_i$ . In this chapter we prove

LEMMA 6.1.  *$F$  is a fundamental domain for the action of  $\varrho(\Gamma)$  on  $\Delta$ . More precisely,*

- (1)  $\Delta = \bigcup_{\gamma \in \varrho(\Gamma)} \gamma(F)$ ,
- (2)  $\gamma(F) \cap F \neq \emptyset$  if and only if  $\gamma \in \{I_0, I_1, I_2\}$ ,
- (3)  $I_j(F) \cap F \subset \partial F$ .

There is an order-3 element  $s_3 \in PU(2, 1)$  such that  $s_3(\widehat{C}_j) = \widehat{C}_{j+1}$ , indices taken mod 3. Since our constructions are natural,  $s_3(\Sigma_j) = \Sigma_{j+1}$ . Let  $G \subset PU(2, 1)$  be the group obtained by adjoining  $s_3$  to  $\varrho(\Gamma)$ . Since  $\varrho(\Gamma)$  has finite index in  $G$ , the two groups have the same limit set and domain of discontinuity. Our proof of Lemma 6.1 involves studying the orbit  $G(\Sigma_0)$ . Note that  $G(\Sigma_0) = G(\Sigma_1) = G(\Sigma_2)$ .

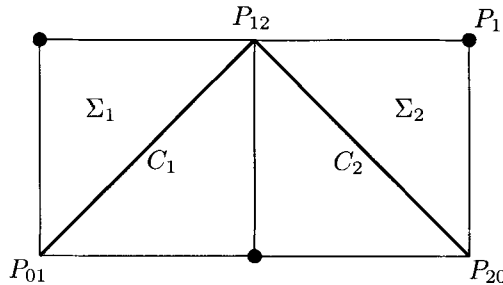


Fig. 11

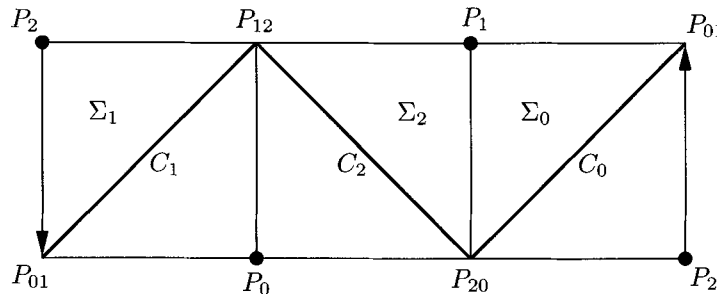


Fig. 12

**6.2. The pattern of tangencies**

Figure 11 shows a schematic picture of  $\Sigma_1$  and  $\Sigma_2$ . One must imagine that each of these spheres is the double of a square, and has been flattened down onto the plane, for the purposes of drawing.

The equators of the two spheres appear as thickened diagonal arcs. The arc of tangency appears as a vertical arc.

Figure 12 shows a schematic picture of all three spheres. The spheres  $\Sigma_0$  and  $\Sigma_1$  are not shown tangent. The free vertical arc of  $\Sigma_0$  is glued to the free vertical arc of  $\Sigma_1$  in the manner indicated by the arrows. The union of the three balls  $B_0 \cup B_1 \cup B_2$  resembles a Möbius band, which has been fattened up in three segments. One could picture three pieces of ravioli stuck together, end to end, to approximate a Möbius band. The balls are the filling of the ravioli, and the spheres are the dough.

One creates  $F$  by taking the closure of the complement of this thickened Möbius band, and deleting the six distinguished points.

*Remark.* The reader who is anxious to get to the topology of  $\Delta/\rho(\Gamma)$  can assume Lemma 6.1 and skip to §7 at this point.

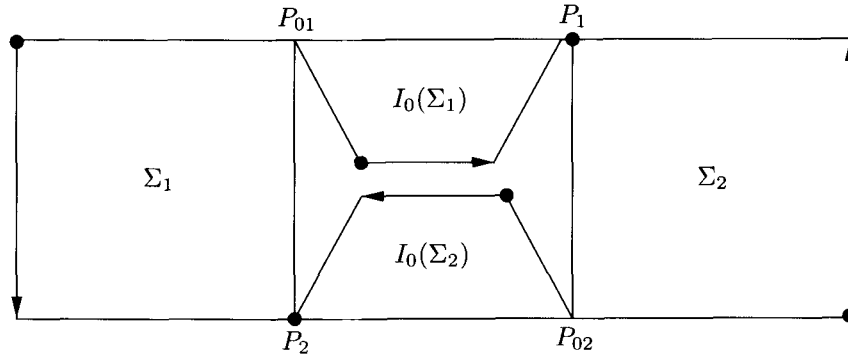


Fig. 13

**6.3. Pictures of the orbit**

Say that a sphere  $\omega'' \in G(\Sigma_0)$  separates the spheres  $\omega, \omega' \in G(\Sigma_0)$  if there are open balls  $B, B'$  bounded by  $\omega, \omega'$  such that  $B$  and  $B'$  are contained in different components of  $S^3 - \omega''$ . To avoid trivialities, we insist that all three spheres are distinct. We write  $\delta(\omega, \omega') = n + 1$  if there are  $n$  distinct spheres in  $G(\Sigma_0)$  which separate  $\omega$  from  $\omega'$ . We say that  $\omega$  and  $\omega'$  are adjacent if and only if  $\delta(\omega, \omega') = 1$ , and separated otherwise. It follows from symmetry and from the argument in Corollary 4.2 that:

(1)  $\Sigma_0$  is adjacent to  $\Sigma_i$  and  $I_0(\Sigma_j)$  for  $i, j \in \{1, 2\}$ .

(2) If  $\omega \neq \Sigma_0$  is not one of the four spheres listed in (1), then  $\Sigma_0$  and  $\omega$  are separated.

Indeed, one of these four spheres separates  $\omega$  from  $\Sigma_0$ .

(3) If  $\delta(\omega, \omega') = 2$  then there is some  $\gamma \in G$  and indices  $i, j \in \{1, 2\}$  such that  $\gamma(\omega) = \Sigma_i$  and  $\gamma(\omega') = I_0(\Sigma_j)$ . (Proof: Apply an element which moves the separating sphere to  $\Sigma_0$ .)

(4) If  $\delta(\omega, \omega') = 2$  and  $\omega \cap \omega' \neq \emptyset$  then  $\omega \cap \omega'$  is a single point which is  $G$ -equivalent to one of the six special points on  $\Sigma_0 \cup \Sigma_1 \cup \Sigma_2$ . (Proof: Move the separating sphere to  $\Sigma_0$  and observe that  $\Sigma_0 \cap \omega$  and  $\Sigma_0 \cap \omega'$  are foliating arcs of different hemispheres.)

Figure 13 shows  $\Sigma_0$  and its four adjacent spheres. We have depicted  $\Sigma_0$  as a transparent doubled square. The two spheres  $\Sigma_1$  and  $\Sigma_2$ , represented by large quadrilaterals, are on the “outside” of  $\Sigma_0$  in the sense that the reader could touch these spheres without penetrating  $\Sigma_0$ . The two spheres  $I_0(\Sigma_1)$  and  $I_0(\Sigma_2)$  are represented by doubles of small quadrilaterals. These spheres are “inside”  $\Sigma_0$  in the sense that the reader must penetrate  $\Sigma_0$  in order to touch a generic point of these spheres. The outer spheres are glued together, and the inner spheres are glued together, as indicated by the arrows. The black dots denote the poles of the spheres. The equators are not drawn, but can be determined from the positions of the poles.

Figure 14 fills in all the spheres adjacent to those in Figure 13. The new spheres are again represented by doubled quadrilaterals. Nearby parallel edges are glued as indicated

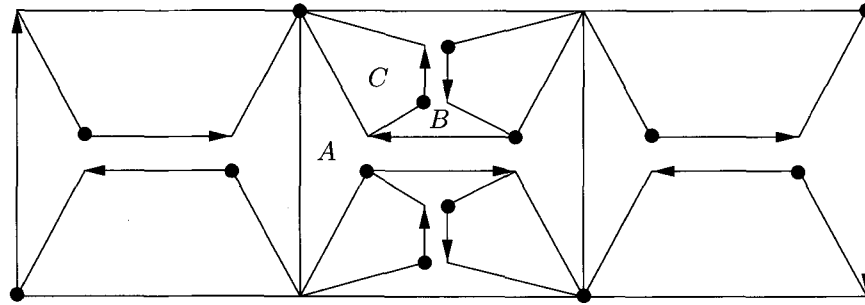


Fig. 14

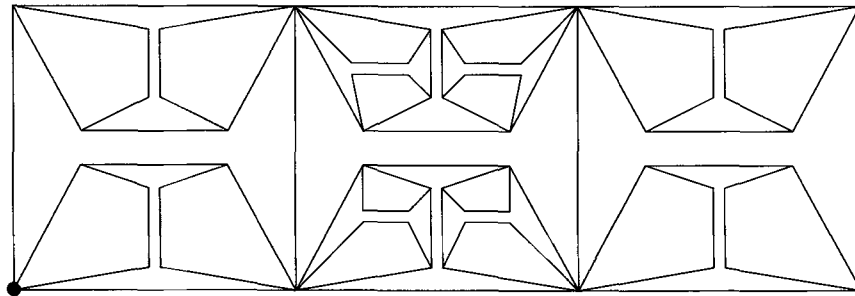


Fig. 15

by the arrows. The larger spheres separate the reader from the smaller ones. For instance, in order to touch generic points of the sphere labelled  $C$ , the reader must penetrate the sphere labelled  $B$ . In order to touch generic points of the sphere labelled  $B$ , the reader must penetrate the sphere  $A$ .

Figure 15 fills in all the spheres adjacent to those shown in Figure 14. The gluing arrows and the black dots have been deleted to give a less cluttered picture. Once a single black dot has been placed, all the other black dots, as well as the arrows, are forced.

#### 6.4. The neighborhood of a vertex

Figure 16 shows the pattern made by the union of spheres which contain a single point  $x$ . Spheres are represented as in the other pictures, with the larger spheres separating the reader from the smaller spheres.

The pattern of spheres is the same whether or not  $x$  is a pole. The labelling, however, is different in the two cases. The two representative cases are  $x=P_{12}$  and  $x=P_0$ .

When  $x=P_{12}$ , the fixed point of  $I_1I_2$ , the spheres are

$$\dots, I_1I_2I_1(\Sigma_2), I_1I_2(\Sigma_1), I_1(\Sigma_2), \Sigma_1, \Sigma_2, I_2(\Sigma_1), I_2I_1(\Sigma_2), I_2I_1I_2(\Sigma_1), \dots$$

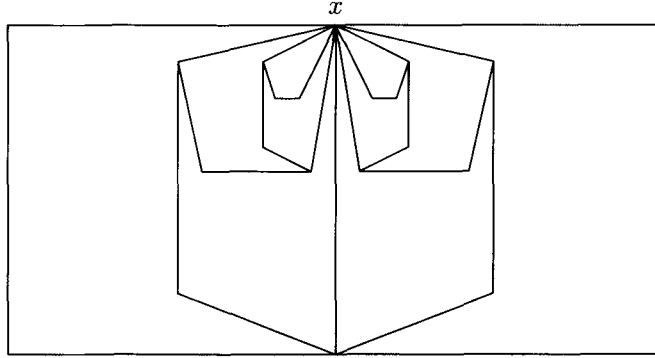


Fig. 16

When  $x=P_0$ , the fixed point of  $I_1I_0I_2$ , the spheres are

$$\dots, I_1I_0I_2(\Sigma_1), I_1I_0(\Sigma_2), I_1(\Sigma_0), \Sigma_1, \Sigma_2, I_2(\Sigma_0), I_2I_0(\Sigma_1), I_2I_0I_1(\Sigma_2), \dots$$

In both cases, we have listed these spheres so that they are adjacent if and only if they are listed successively.

Both sequences above are doubly infinite. Later in the chapter, it will be useful to work with the singly infinite sequences

$$\Sigma_2, I_2(\Sigma_1), I_2I_1(\Sigma_2), I_2I_1I_2(\Sigma_1), I_2I_1I_2I_1(\Sigma_2), \dots, \quad (33)$$

$$\Sigma_2, I_2(\Sigma_0), I_2I_0(\Sigma_1), I_2I_0I_1(\Sigma_2), I_2I_0I_1I_2(\Sigma_0), \dots \quad (34)$$

### 6.5. Proof modulo shrinking

Say that a sequence  $S=\{\omega_n\} \in G(\Sigma)$  is *nested* if there is a sequence of balls  $\{B_n\}$  such that  $B_n \supset B_{n+1}$  and  $\omega_n$  bounds  $B_n$ , for all  $n$ . In this case, we say that  $\{\omega_n\}$  is *good* if the infinite intersection  $\bigcap \bar{B}_n$  is a single point. Following this section, most of the chapter is devoted to proving

LEMMA 6.2 (Shrinking). *All infinite nested sequences are good.*

We now establish Lemma 6.1. Let  $F^\circ$  be the interior of  $F$ . Note that  $F-F^\circ \subset \Sigma_0 \cup \Sigma_1 \cup \Sigma_2$ . The proof of Corollary 4.2 shows that  $\gamma(F^\circ) \cap F^\circ = \emptyset$  for any nontrivial  $\gamma \in \varrho(\Gamma)$ . This gives statement (3) of Lemma 6.1.

The analysis in the previous section shows that  $\Sigma_0$  intersects any nonadjacent sphere in one of the points  $P_1, P_2, P_{01}, P_{02}$ . Cyclically permuting the indices, we get the following result: For any nontrivial  $\gamma \notin \varrho(\Gamma) - \{I_0, I_1, I_2\}$ , the intersection  $\gamma(\Sigma_i) \cap \Sigma_j$  is contained in

one of the six points  $\bigcup P_{nm} \cup \bigcup P_k$ . Thus  $\gamma(F - F^o) \cap (F - F^o) = \emptyset$  for such  $\gamma$ . Combining this with  $\gamma(F^o) \cap F^o = \emptyset$  gives statement (2) of Lemma 6.1.

Let

$$\Delta' = \bigcup_{\gamma \in \varrho(\Gamma)} \gamma(F).$$

Statement (2) of Lemma 6.1 implies that every point of  $F$  has an open neighborhood which intersects only finitely many  $\varrho(\Gamma)$ -translates of  $F$ . By symmetry, this is true for all points in  $\Delta'$ . Hence,  $\Delta' \subset \Delta$ .

Let  $p \in S^3 - \Delta'$ . Suppose first that  $p$  is  $\varrho(\Gamma)$ -equivalent to some  $P_{ij}$  or to some  $P_k$ . Since  $\Lambda$  contains the fixed points of elements of  $\varrho(\Gamma)$  we have  $p \in \Lambda$ . The other possibility is that  $p \in S^3 - \Delta''$ , where

$$\Delta'' = \bigcup_{\gamma \in \varrho(\Gamma)} \gamma(\bar{F}).$$

Here  $\bar{F} = S^3 - \bigcup B_j$ . In this case, there is an infinite nested sequence  $\{\omega_n\}$  such that (in the notation above)  $p \in \bigcap \bar{B}_n$ . Each  $\Sigma_j$  has two poles. We choose one pole arbitrarily and call it  $p_j$ . By the Shrinking Lemma,  $p = \bigcap \bar{B}_n$ , and hence  $p_j \rightarrow p$ . Note that  $p_j \in \Lambda$ , since  $p_j$  is a parabolic fixed point. Since  $\Lambda$  is closed,  $p \in \Lambda$ . In both cases considered, we have  $S^3 - \Delta' \subset \Lambda$ . Hence,  $\Delta \subset \Delta'$ . Combining this with the other containment, we get  $\Delta = \Delta'$ . This is statement (1) of Lemma 6.1.  $\square$

## 6.6. Proof of the Shrinking Lemma

Say that a nested sequence  $S$  is *maximal* if  $S$  is not a proper subsequence of a nested sequence  $S'$  whose first element coincides with  $S$ . For instance, the sequences (33) and (34) are maximal. It clearly suffices to prove the Shrinking Lemma only for maximal nested sequences.

Say that two maximal nested sequences  $S = \{\omega_j\}$  and  $S' = \{\omega'_j\}$  *stably agree* if there are indices  $n$  and  $n'$  such that  $\{\omega_j \mid j > n\}$  and  $\{\omega'_j \mid j > n'\}$  coincide. More generally, we say that sequences  $S$  and  $S''$  are *equivalent* if there is some element  $g \in G$  such that  $S$  and  $S' = g(S'')$  stably agree. If  $S$  and  $S'$  are equivalent, and  $S'$  is good, then so is  $S$ .

Say that the maximal nested sequence  $S$  has *Type A* if it is equivalent to sequence (33), and *Type B* if it is equivalent to sequence (34). Otherwise, say that  $S$  has *Type C*. Lemmas 5.2 and 5.1, combined with the remarks about equivalence, say that all sequences of Type A are good and that all sequences of Type B are good. We just have to deal with sequences of Type C.

**LEMMA 6.3.** *Suppose that  $S = \{\omega_n\}$  is a sequence of Type C. Then there is an infinite sequence  $a_0 < b_0 < a_1 < b_1 \dots$ , and elements  $g_1, g_2, \dots \in G$ , such that  $\omega_{a_j} \cap \omega_{b_j} = \emptyset$ ,  $\omega_{a_j} = g_j(\omega_{a_0})$  and  $\omega_{b_j} = g_j(\omega_{b_0})$  for all  $j$ .*

*Proof.* We will use the function  $\delta$ , defined in §6.3. Observe first that there are only finitely many pairs  $(\omega, \omega')$ , modulo the diagonal action of  $G$  on  $G(\Sigma_0) \times G(\Sigma_0)$ , such that  $\delta(\omega, \omega') < N$ , for any  $N$ . (One simply normalizes so that  $\omega = \Sigma_0$ , leaving finitely many choices for  $\omega'$ .) Second, observe that  $P_n = \omega_{n-1} \cap \omega_{n+1}$  is either a point or the empty set, by the analysis in §6.3.

Suppose that  $P_n$  is the empty set, for infinitely many indices  $n_1, n_2, \dots$ . Note that  $\delta(\omega_{n-1}, \omega_{n+1}) = 2$ . Using our first observation, we can take a subsequence so that the pairs  $(\omega_{n_j-1}, \omega_{n_j+1})$  are all equivalent under the diagonal  $G$ -action. We set  $a_j = n_j - 1$  and  $b_j = n_j + 1$ .

Suppose that  $P_n$  is a point for all but finitely many indices. Since  $S$  has Type C, there are infinitely many indices  $m_1, m_2, \dots$  such that  $P_{m_j} \neq P_{m_j+1}$ . Here  $\omega_{m_j-1} \cap \omega_{m_j+2} = \emptyset$  and  $\delta(\omega_{m_j-1}, \omega_{m_j+2}) = 3$ . As above, we can assume that all these pairs are equivalent under diagonal  $G$ -action. We set  $a_j = m_j - 1$  and  $b_j = m_j + 2$ .  $\square$

Suppose that  $\omega$  and  $\omega'$  are embedded spheres, not necessarily disjoint. We define an invariant

$$\mathbf{X}(\omega, \omega') = \inf_{x, y \in \omega} \inf_{x', y' \in \omega'} \mathbf{X}(x, y, x', y').$$

The infimum is taken over quadruples of distinct points. Here we are using the cross ratio, defined in equation (12). Here are two basic properties:

- (1)  $\mathbf{X}(\omega, \omega') = 0$  if and only if  $\omega \cap \omega' = \emptyset$ ,
- (2)  $\mathbf{X}(g(\omega), g(\omega')) = \mathbf{X}(\omega, \omega')$  for any  $g \in PU(2, 1)$ .

LEMMA 6.4. *Let  $S = \{\omega_n\}$  be a maximal nested sequence which is not good. Given any  $\varepsilon > 0$  there is some  $N \in \mathbf{N}$  having the property that  $\mathbf{X}(\Sigma_m, \Sigma_n) < \varepsilon$  if  $m, n > N$ .*

*Proof.* Let  $\{B_j\}$  be the sequence of balls associated to  $S$ , as above. Let  $x \neq y$  be two points in  $\bigcap \bar{B}_j$ . We can find points  $x_j, y_j \in \Sigma_j$  such that  $x_j \rightarrow x$  and  $y_j \rightarrow y$ . The sequence  $\{x_j\}$  is a Cauchy sequence in  $S^3$ , and so is the sequence  $\{y_j\}$ . Also, the limits of these sequences are different. We have  $\mathbf{X}(\Sigma_m, \Sigma_n) \leq \mathbf{X}(x_m, y_m, x_n, y_n)$ . Let  $X_m$  and  $Y_m$  be affine lifts of  $x_m$  and  $y_m$ . Likewise for  $X_n$  and  $Y_n$ . We see that

$$\langle X_m, X_n \rangle \rightarrow 0, \quad \langle Y_m, Y_n \rangle \rightarrow 0,$$

while the other two terms remain uniformly bounded away from 0. Hence, we conclude that  $\mathbf{X}(x_m, y_m, x_n, y_n)$  is vanishingly small for  $m$  and  $n$  increasingly large.  $\square$

Suppose that  $S$  has Type C. Using the notation of Lemma 6.3, we see that  $\mathbf{X}(\omega_{a_j}, \omega_{b_j}) \neq 0$  is a quantity which is independent of  $j$ . In particular, the conclusion of Lemma 6.4 does not hold. Hence  $S$  must be good.



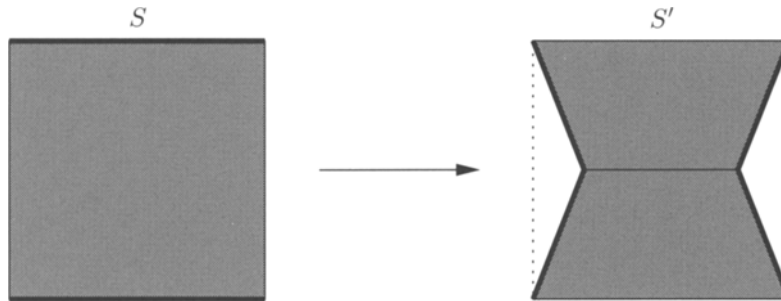


Fig. 17

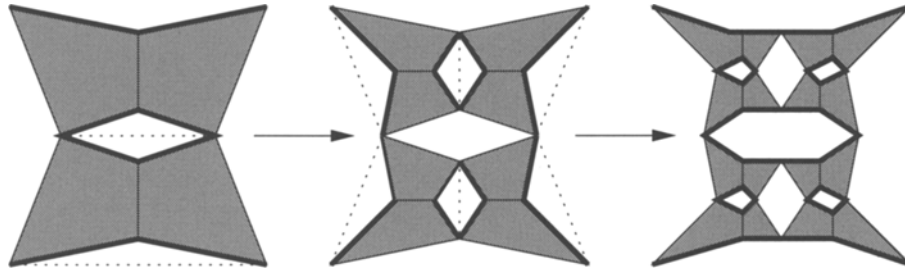


Fig. 18

**6.7. The limit set**

Our description of  $\Lambda$  comes straight from Figures 13–16 and their obvious continuations. First we construct a space  $S_\infty$  which is related to  $\Lambda$ . Then we modify  $S_\infty$  to get  $2S_\infty^\infty$ , which is homeomorphic to  $\Lambda$ .

Given the solid unit square,  $S$ , with top and bottom edges distinguished, let  $S'$  be the union of two solid quadrilaterals shown in Figure 17. Unlike in Figures 13–16, the quadrilaterals here represent themselves, rather than their doubles.

If  $Q$  is a quadrilateral, with a distinguished pair of opposite edges, there is a real projective transformation  $T_Q$  such that  $T_Q(S)=S$ . This map is unique up to order-2 rotation. We define  $Q'=T(S')$ .

Let  $S_0=S$  and  $S_1=S'$ . Note that  $S_1$  is the union of two quadrilaterals,  $S_{11}\cup S_{12}$ . Define  $S_2=S'_{11}\cup S'_{12}$ . Figure 18 shows how the pattern continues to get nested sets  $S_1\supset S_2\supset S_3 \dots$ . Define  $S_\infty=\bigcap S_k$ .

We now modify  $S_\infty$  recursively. We color the four outer vertices of  $S_\infty$  alternately white and black, as shown in Figure 19. Note that  $S_\infty$  is the union  $TS_\infty\cup BS_\infty$  of two homeomorphic copies of itself. Here  $TS_\infty\cap BS_\infty$  is two vertices.

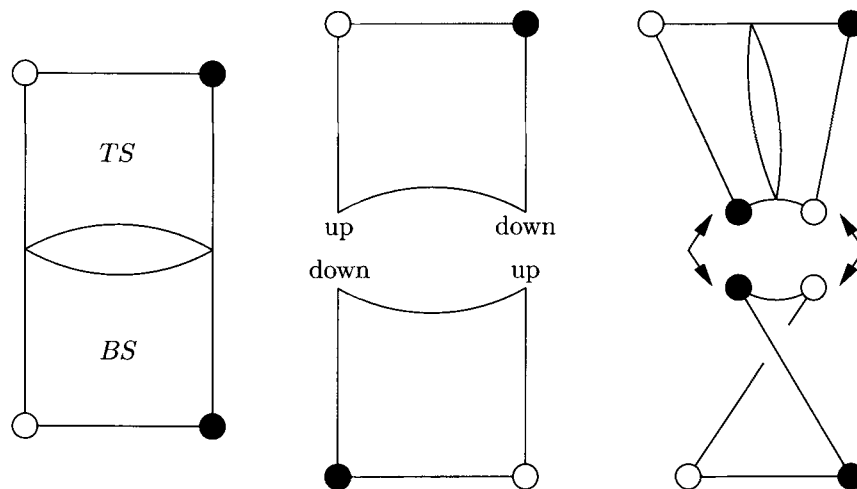


Fig. 19

(1) Cut  $S_\infty$  open along the two vertices  $TS_\infty \cap BS_\infty$ .

(2) Twist  $TS_\infty$  90 degrees clockwise out of the plane, by pulling one of the cut vertices up and pushing the other one down. Likewise twist  $BS_\infty$ .

(3) Glue the twisted copies together along their two nearby vertices.

Call the resulting object  $S_\infty^1$ . After having made this modification, we color two additional vertices of  $S_\infty^1$  alternately black and white, as shown.

Note that  $S_\infty^1$  is a union of two twisted copies of  $TS_\infty$  and  $BS_\infty$ . The outer vertices of each half are already colored alternately black and white. We may perform the same kind of twist modification on each of these halves, keeping the outer vertices fixed in the process. (The right part of Figure 19 shows one of the pieces which is to be twisted. The other piece is difficult to draw.) Call the result  $S_\infty^2$ . After the modification is done, we can color four additional vertices alternately white and black. In general,  $S_\infty^n$  is a union of  $2^n$  twisted copies of  $S_\infty$ , and each of these copies has its four outer vertices colored alternately white and black. One creates  $S_\infty^{n+1}$  by modifying each copy as above. Let  $S_\infty^\infty$  be the limit of this process.

Let  $2S_\infty^\infty$  denote the space obtained by gluing two copies of  $S_\infty^\infty$ , along the outermost four vertices, with a 90 degree twist.  $2S_\infty^\infty$  is homeomorphic to  $\Lambda$ . Indeed, if all twists are made in a clockwise way, then the embedding is correct. The homeomorphism extends to all of  $S^3$ .

There is a countable collection of vertices of  $2S_\infty^\infty$  colored white, and a countable collection colored black. The union of each type of vertices is dense in  $2S_\infty^\infty$ . Our homeomorphism carries the black vertices to fixed points of elements conjugate to  $I_1 I_0 I_2$ , and the white vertices to fixed points of elements conjugate to  $I_1 I_2$ .

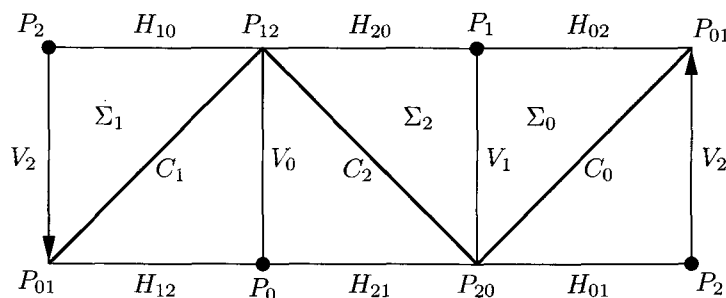


Fig. 20

### 7. Topology of the quotient

#### 7.1. The pattern of tangencies

This section is a continuation of §6.2.

It is convenient to define

$$V_0 = \Omega(E_0, P_0; P_{12}) = \Sigma_1 \cap \Sigma_2.$$

The arcs  $V_1$  and  $V_2$  are defined by cyclically permuting the indices. For all  $i \neq j$ , the arcs  $V_i$  and  $V_j$  are foliating arcs of different hemispheres of the same hybrid sphere. Also, the endpoints of these arcs differ. Hence,  $V_i \cap V_j = \emptyset$ .

Figure 20 is a repeat of Figure 12, with additional labels drawn in. For  $i \neq j$  we define

$$H_{ij} = I_i(V_j).$$

The four arcs  $H_{01}, V_1, H_{02}, V_2$  intersect in the same topological pattern as a square. Let  $S_0$  be this topological square. Note that  $S_0$  is a closed circuit on  $\Sigma_0$  which divides  $\Sigma_0$  into two disks, each of which has, as a “diagonal”, part of  $C_0$ , the equator of  $\Sigma_0$ . These diagonals further divide each of the disks into two topological triangles. One of the two disks, and two of the triangles, is visible in Figure 20. The other disk, and the other two triangles, are hiding behind the ones shown. By cyclically permuting the indices, we see that the same picture takes place in each of the three hybrid spheres. Thus,  $\partial(B_0 \cup B_1 \cup B_2)$  has a triangulation into twelve triangles.

#### 7.2. The face pairings

Let  $F$  be as in equation (32). We spend the rest of the chapter deducing Theorem 1.2 from Lemma 6.1.

We have already seen above that  $\partial(B_0 \cup B_1 \cup B_2)$  has a triangulation into twelve triangles.  $\partial F$  has the same triangulation. The vertices are deleted. (Note the analogy

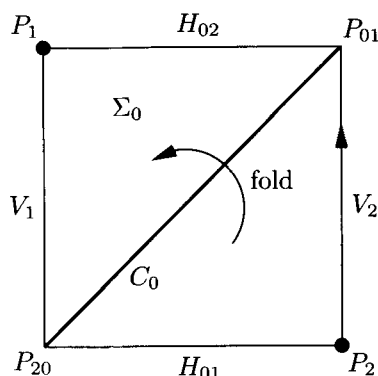


Fig. 21

with an ideal hyperbolic triangle.) The elements  $I_0$ ,  $I_1$  and  $I_2$  identify the triangles in pairs. Each element identifies two pairs of triangles.

Recall from the previous section that  $S_0$  is the circuit on  $\Sigma_0$  which divides it into two solid squares, each of which is a union of two triangles, separated by an arc of  $C_0$ . The element  $I_0$  identifies these triangles in pairs, by folding along the arc of  $C_0$ , as shown in Figure 21. The same fold takes place on the back side of the hybrid sphere.

Let  $Q$  be the quotient of  $F$  by its face pairings. We can use the information given in this section to deduce the homeomorphism type of  $Q$ . The rest of the chapter is devoted to this enterprise.

### 7.3. Topology of the quotient

For the purposes of visualizing  $Q$ , we equip  $S^3$  with the round metric. Let  $B_\varepsilon$  be the  $\varepsilon$ -tubular neighborhood of  $B_0 \cup B_1 \cup B_2$ , for some extremely small  $\varepsilon$ . (It is useful to think of  $\varepsilon$  as infinitesimally small.) There is an obvious nearest point map  $\phi: \partial B_\varepsilon \rightarrow \partial(B_0 \cup B_1 \cup B_2)$ . Define

$$\tilde{F} = S^3 - B_\varepsilon - \bigcup \phi^{-1}(P_i) - \bigcup \phi^{-1}(P_{jk}).$$

If  $\varepsilon$  is sufficiently small then  $B_\varepsilon$  is homeomorphic to an open solid torus. Therefore,  $\tilde{F}$  is a solid torus with six points deleted from its boundary.

Pulling back by  $\phi^{-1}$ , the triangulation of  $\partial(B_0 \cup B_1 \cup B_2)$  induces a triangulation on  $\partial\tilde{F}$ . Forgetting about indices, the edges on  $\partial\tilde{F}$  are labelled by  $\tilde{H}$ ,  $\tilde{V}$  and  $\tilde{C}$ . The map  $\phi$  is one-to-one on the open triangles, the  $\tilde{C}$ -edges and the  $\tilde{H}$ -edges. On the  $\tilde{V}$ -edges, however,  $\phi$  is two-to-one.

The triangles on  $\partial\tilde{F}$  are identified, in pairs, by folding across the  $\tilde{C}$ -edges. We will see that the face pairings on  $\partial\tilde{F}$  automatically identify all the  $\tilde{V}$ -edges which are

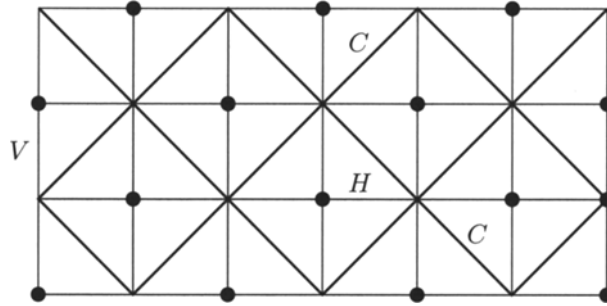


Fig. 22

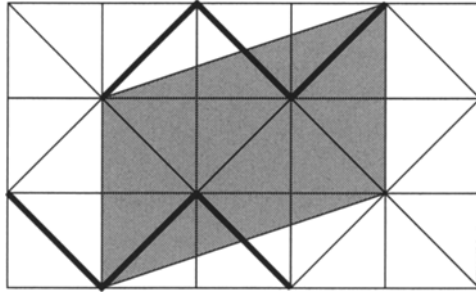


Fig. 23

identified by  $\phi$ . Thus, the quotient of  $\tilde{Q}$  of  $\tilde{F}$  by its face pairings is homeomorphic to  $Q$ .

Let  $\partial_* \tilde{F}$  be the torus which is obtained by filling in the punctures on  $\partial \tilde{F}$ .  $\mathbf{R}^2$  universally covers  $\partial_* \tilde{F}$ . This covering induces a cover of  $\partial \tilde{F}$  by  $\mathbf{R}^2 - \mathbf{Z}^2$ . The triangulation of  $\partial \tilde{F}$  lifts to a triangulation of  $\mathbf{R}^2 - \mathbf{Z}^2$ . The vertices of the squares belong to  $\mathbf{Z}^2$ . Half of these vertices, which are colored black, project to the points  $\tilde{P}_i$ . The other half project to the points  $\tilde{P}_{jk}$ . The pattern comes straight from Figure 20.

The triangulation on  $\partial \tilde{F}$  is obtained from the triangulation of  $\mathbf{R}^2 - \mathbf{Z}^2$  by taking the quotient by the deck group of the covering. Specifying the deck group of the covering amounts to placing a parallelogram  $\Pi$  in Figure 22, and agreeing that the deck group is generated by identifying the opposite sides of  $\Pi$  by translations.

Since  $\partial \tilde{F}$  is triangulated by twelve triangles, and each triangle has area  $\frac{1}{2}$ , we see that  $\Pi$  must have area six. If we follow two consecutive  $\tilde{V}$ -edges, we trace out a closed loop on the solid torus containing  $\partial \tilde{F}$ . Indeed, such loops are mapped to the  $V_j$ , in two-to-one fashion. Looking at Figure 20, we see that a horizontal zigzag pattern made from three successive  $\tilde{C}$ -edges makes a closed loop. Figure 23 shows pictures of the vertical loops and the horizontal zigzag loops. We deduce that the shaded parallelogram serves as valid choice for  $\Pi$ .

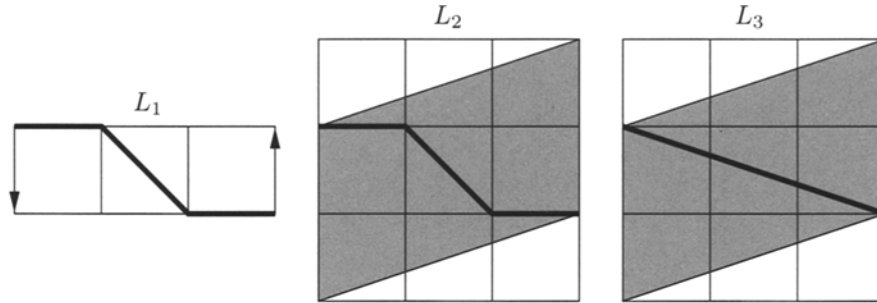


Fig. 24

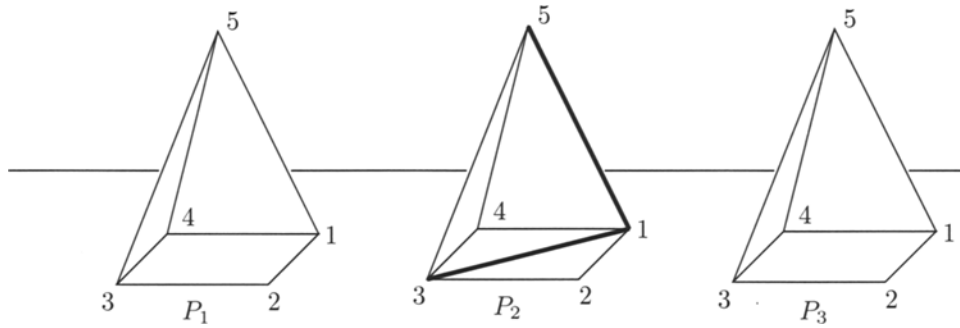


Fig. 25

Recalling that the triangular faces of  $\partial\tilde{F}$  are identified in pairs by folding along the diagonal edges, we see that consecutive vertical edges in  $\partial\tilde{F}$  are automatically identified. Thus, the face pairings on  $\partial\tilde{F}$  automatically identify the  $\tilde{V}$ -edges which are also identified under  $\phi$ , as we had claimed above.

It remains to figure out which loops on  $\partial\tilde{F}$  are contractible in  $\tilde{F}$ . The left-hand side of Figure 24 shows a loop  $L_1$  on  $X=B_0\cup B_1\cup B_3$  which is contractible in  $S^3-X$ . We omit the proof of this statement. The reader can perform the proof by lightly gluing a piece of string to a Möbius band, along  $L_1$ , and observing that one can pull the string off the Möbius band.

The middle part of Figure 24 shows the loop  $L_2\in\partial_*\tilde{F}$  which maps to  $L_1$  under our nearest point map. Curves isotopic to  $L_2$  are contractible in  $\tilde{F}$ . The curve  $L_3$  is isotopic to  $L_2$  in  $\partial_*\tilde{F}$ . Curves in  $\partial\tilde{F}$ , which are parallel to  $L_3$ , contract in  $\tilde{F}$ .

Now we introduce some hyperbolic geometry. Let  $P\subset\mathbf{H}^3$  be the regular ideal pyramid with ideal square base, created by cutting in half the regular ideal octahedron. Let  $\{P_n|n\in\mathbf{Z}\}$  be an infinite collection of isometric copies of  $P$ , all labelled as in Figure 25.

Let  $P_{ij}$  be the  $j$ th point of  $P_i$ . Let  $(n;ijk)$  be the triangle of  $P_i$  whose vertices are  $P_{ni}, P_{nj}$  and  $P_{nk}$ . We form the space  $\Omega$  by gluing the face  $(n+1, 543)$  to the face  $(n, 125)$ ,

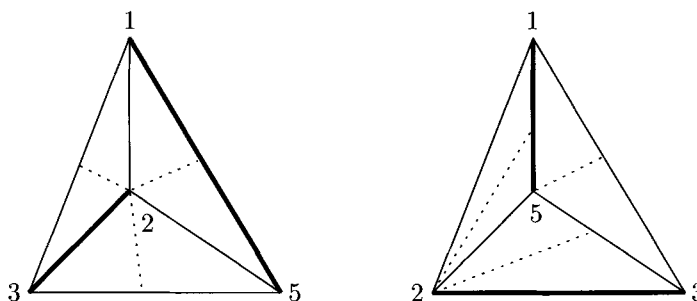


Fig. 26

for all  $n \in \mathbf{Z}$ . Our notation is such that  $P_{n+1,5}$  is glued to  $P_{n1}$ , etc. One can visualize this space by lining up the pyramids along an axis, as shown in Figure 25, twisting  $P_n$  by a rotation of  $\frac{2}{3}\pi n$ , and then sliding the pyramids together.

$\partial\Omega$  consists entirely of ideal squares. Half of these squares, which we call *Type A*, are the bases of the pyramids. Let  $D_A(n)$  be the diagonal joining  $P_{n1}$  and  $P_{n3}$ . We call  $D_A(n)$  a *diagonal of Type A*. The other ideal squares are formed by the unions of the form  $(n, 145) \cup (n+1, 235)$ . We call these ideal squares of *Type B*. We call the edge  $D_B(n) = (n, 145) \cap (n+1, 235)$  a *diagonal of Type B*. Note that  $D_B(n)$  joins the points  $P_{n1}$  and  $P_{n5}$ . Figure 25 shows  $D_A(2)$  and  $D_B(2)$ , drawn with thick lines. The pattern of distinguished diagonals on  $\partial\Omega$  looks locally just like the pattern of diagonals in Figure 22.

There is an isometry  $I: \Omega \rightarrow \Omega$  such that  $I(P_n) = P_{n+1}$ . The quotient  $\Omega/I^3$  is a solid torus with six deleted vertices whose boundary has the same combinatorial structure as  $\partial\tilde{F}$ . Under a suitable choice of identification, the square base of  $P_0$  is identified to the circuit  $S_0$  shown in Figure 20. The element  $I$  has the same action on  $\Omega/I^3$  as the element  $s_3$  has on  $\tilde{F}$ .

It is easily checked that  $R_0(\Sigma_0) = \Sigma_0$ , and that  $R_0$  acts as 180 degree rotation about the circuit  $S_0$ . Rotating 180 degrees about the axis of the pyramid  $P_0$  extends to an isometry  $R$  of  $\Omega$ . The element  $R$  has the same action on  $\Omega/I^3$  as  $R_0$  has on  $\partial\tilde{F}$ .

Recall that  $G$  is obtained by adjoining  $s_3$  to  $\varrho(\Gamma)$ . If we let  $\mu$  be the group action on  $S^3$  obtained by adjoining  $R_0$  to  $G$  then  $\Delta/\mu$  is homeomorphic to the quotient of  $W = \Omega/(I, R)$  by the identifications induced by folding across the distinguished diagonals.

A fundamental domain for  $W$  is one half of  $P_0$ . We may take this half to be an ideal tetrahedron  $T$  whose vertices are  $P_{01}$ ,  $P_{02}$ ,  $P_{03}$  and  $P_{05}$ . Let  $F_A$  be the fold across  $D_A(0)$ . We have

$$\begin{aligned} F_A \circ R(0; 123) &= F_A(0; 341) = (0; 321), \\ R \circ I(0; 125) &= R \circ I(1; 543) = R(0; 543) = (0; 521), \\ I \circ D_B \circ R(0; 325) &= I \circ D_B(0; 145) = I(1; 523) = (0; 523). \end{aligned}$$

Thus, each face of  $T$  is identified to itself by a fold across a bisecting edge. The pattern is as shown in Figure 26. (Two views are shown, so that one can see all fold lines.) The thin edges correspond to dihedral angles of  $\frac{1}{2}\pi$ , and the thick edges correspond to dihedral angles of  $\frac{1}{4}\pi$ . The dotted edges are the fold lines.

The points 1, 3, 5 all get identified to each other, and 2 is only identified to itself. Comparing the treatment of the Whitehead link complement in  $\Sigma^3 - L$  in [Th, pp. 129–131], one can see that  $W = (\Sigma^3 - L)/D_4$ . This completes the proof of Theorem 1.1.  $\square$

## 8. The topological conjugacy

### 8.1. Main construction

Let  $\varrho_s: \Gamma \rightarrow PU(2, 1)$  be the representation with angular invariant  $s \in [0, \bar{s})$ . We can generate  $\varrho_s$  simply by replacing  $\lambda$ , defined in §4.1, with the variable

$$\lambda_s = \frac{s+i}{\sqrt{2+2s^2}}. \quad (35)$$

Setting  $\bar{s} = \sqrt{125/3}$  yields the constant  $\lambda$  used in §4.1. We get matrices  $I_{j,s}$  by using  $\lambda_s$  in place of  $\lambda$  in equation (15). The representation  $\varrho_s$  is given by  $\varrho_s(i_j) = I_{j,s}$ . We will suppress the subscript  $\bar{s}$ . For instance,  $I_j = I_{j,\bar{s}}$ .

It is easy to see, and it is proved in [S], that:

- (1)  $I_{j,s}$  converges to  $I_j$  as  $s \rightarrow \bar{s}$ .
- (2)  $g_s = I_{1,s} I_{0,s} I_{2,s}$  converges to  $g$  as  $s \rightarrow \bar{s}$ .
- (3) Conjugation by  $R_0$  interchanges  $I_{1,s}$  and  $I_{2,s}$ , and also preserves  $I_{0,s}$ .
- (4)  $g_s$  preserves two points  $O_s$  and  $Q_s$ , both of which converge to  $P_0$  as  $s \rightarrow \bar{s}$ .
- (5) The  $\mathbf{C}$ -circle  $E_{0,s}$  containing  $O_s$  and  $Q_s$  converges to  $E_0$  as  $s \rightarrow \bar{s}$ .

Let  $\widehat{C}_{j,s}$  be the chain fixed by  $I_{j,s}$ . Let  $P_{ij,s} = C_{i,s} \cap C_{j,s}$ . Let  $P_{0,s}$  be the arc of  $E_{0,s}$ , bounded by  $O_s$  and  $Q_s$ , which varies continuously with  $s$  and shrinks to  $P_0$  as  $s \rightarrow \bar{s}$ . Define

$$\Sigma_{0,s} = \Sigma(E_{0,s}, P_{0,s}; \widehat{C}_{0,s}).$$

Here  $\Sigma_{0,s}$  is a loxodromic hybrid sphere. We define  $\Sigma_{j,s}$  for  $j=1, 2$  by cyclically permuting the indices.

In §9 we will prove a local version of the Disjointness Lemma.

**LEMMA 8.1.** *There is some  $\varepsilon > 0$  having the following property. Let  $U_\varepsilon$  denote the  $\varepsilon$ -neighborhood of  $P_{12}$ , as measured in the round metric in  $S^3$ . For  $s \in (\bar{s} - \varepsilon, \bar{s})$ , we have  $\Sigma_{1,s} \cap \Sigma_{2,s} \cap U_\varepsilon = \Omega(E_{0,s}, P_{0,s}; P_{12,s}) \cap U_\varepsilon$ .*



COROLLARY 8.2. *There is some  $\delta > 0$  having the following property. For  $s \in (\bar{s} - \delta, \bar{s})$ , we have  $\Sigma_{1,s} \cap \Sigma_{2,s} = \Omega(E_{0,s}, P_{0,s}; P_{12,s})$ .*

*Proof.* Since  $\Sigma_{j,s} \rightarrow \Sigma_j$  as  $s \rightarrow \bar{s}$ , it suffices to prove that there is some  $\delta > 0$  with the following property. If  $V_\delta$  is the  $\delta$ -neighborhood of  $\Sigma_1 \cap \Sigma_2$ , as measured in the round metric, then for  $s \in (\bar{s} - \delta, \bar{s})$ ,

$$\Sigma_{1,s} \cap \Sigma_{2,s} \cap V_\delta = \Omega(E_{0,s}, P_{0,s}; P_{12,s}) \cap V_\delta.$$

This is what we will prove.

From the original Disjointness Lemma, we have

$$\Sigma_1 \cap \Sigma_2 = \Omega(E_0, P_0; P_{12}).$$

Let  $U = U_\epsilon$  be the set from Lemma 8.1. Let  $\Omega_{j,s}$  be the hemisphere of  $\Sigma_{j,s}$  which has  $(E_{0,s}, P_{0,s})$  as a spine. Let  $\Omega'_{j,s}$  be the other hemisphere. If the conclusion of this lemma is false then we may find

$$p_n \in \Sigma_{1,n} \cap \Sigma_{2,n} - U$$

such that  $p_n \rightarrow \Sigma_1 \cap \Sigma_2$ . Here  $s_n \rightarrow \bar{s}$ , and we have set  $\Sigma_{j,s_n} = \Sigma_{j,n}$ , for notational convenience.

On a subsequence we may assume that  $p_n \rightarrow p \in \Sigma_1 \cap \Sigma_2$ . Since  $p \notin U$ , we see that  $p$  is an interior point of  $\Omega_j$  for  $j=1, 2$ . In particular,  $p \notin \Omega'_1 \cup \Omega'_2$ . We conclude that  $p_n \in \Omega_{1,n} \cap \Omega_{2,n}$  for sufficiently large  $n$ .

Let  $\alpha_{j,n}$  be the foliating arc of  $\Omega_{j,n}$  which contains  $p_n$ . Note first that, for  $j=1, 2$ ,

$$\alpha_{j,n} \rightarrow \Sigma_1 \cap \Sigma_2.$$

Also, since  $\alpha_{1,n}$  and  $\alpha_{2,n}$  are defined relative to a common spine, these arcs lie on a common  $\mathbf{R}$ -circle, and have a common endpoint. Hence we have either  $\alpha_{1,n} \subset \alpha_{2,n}$ , or the reverse. Without loss of generality, suppose that  $\alpha_{1,n} \subset \alpha_{2,n}$ . In this case, let  $q_n$  be the endpoint of  $\alpha_{1,n}$  contained on the equator of  $\Omega_{1,n}$ . By construction,  $q_n \in \Omega_{1,n} \cap \Omega_{2,n}$  and  $q_n \rightarrow P_{12}$ . Eventually  $q_n \in U$ , contradicting Lemma 8.1.  $\square$

### 8.2. The pattern of tangency

We will henceforth assume that  $s \in (\bar{s} - \delta, \bar{s})$ . By Lemma 8.2, we have  $\Sigma_{1,s} \cap \Sigma_{2,s} = \Omega(E_{0,s}, P_{0,s}; P_{12,s})$ . One endpoint of this arc is contained in  $P_{0,s}$ . Call this endpoint  $a_s$ . The intersection  $I_{2,s}(\Sigma_{0,s}) \cap \Sigma_{1,s}$  is also an arc, one of whose endpoints,  $b_s$ , is contained in  $P_{0,s}$ . A key difference between the parabolic and loxodromic cases is that  $a_{\bar{s}} = b_{\bar{s}}$ , whereas:

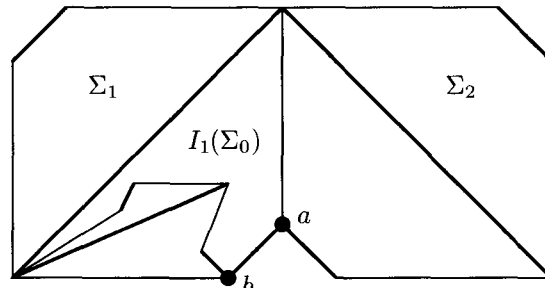


Fig. 27

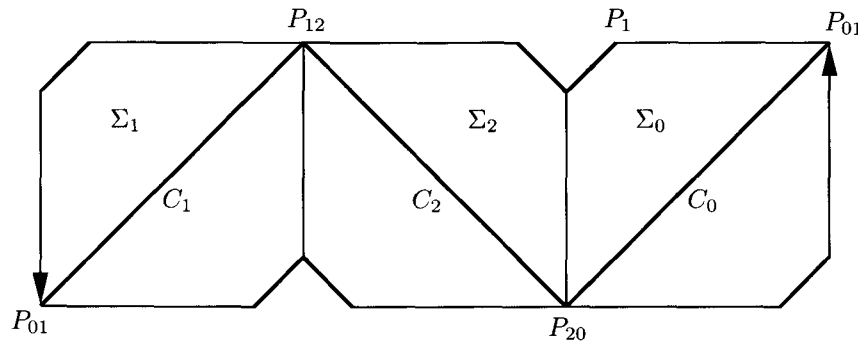


Fig. 28

LEMMA 8.3.  $a_s \neq b_s$  for  $s < \bar{s}$  sufficiently close to  $\bar{s}$ .

*Proof.* If  $a_s = b_s$ , then this common point is fixed by  $g_s$ . Hence, this point must be either  $O_s$  or  $Q_s$ . By construction,  $O_s$  and  $Q_s$ , the endpoints of  $P_{0,s}$ , are not contained in the hemisphere  $\Omega_s = \Omega(E_{0,s}, P_{0,s}; \widehat{C}_{1,s})$ . Since the point  $P_0$  is disjoint from the hemisphere  $I_1(\Omega(E_0, P_0; \widehat{C}_1))$ , the entire arc  $P_{0,s}$ , including the endpoints, is disjoint from the hemisphere  $I_{1,s}(\Omega_s)$  for  $s$  sufficiently close to  $\bar{s}$ .  $\square$

We will represent  $\Sigma_{1,s}$  by the double of a hexagon, as shown in Figure 27. Figure 27 also shows  $\Sigma_{2,s}$ , as well as  $I_1(\Sigma_{0,s})$ . The long diagonals represent the equators of the spheres, as in Figure 11. One of the short thick diagonals on  $\Sigma_1$  represents the arc on  $P_{0,s}$  which joins  $a_s$  to  $b_s$ . The other short thick diagonal on  $\Sigma_{1,s}$  represents the symmetrically located arc, on the other hemisphere.

Figure 28 shows  $\Sigma_{j,s}$ , for  $j=0, 1, 2$ .

Compare Figure 28 with Figure 12, which shows the parabolic case. As  $s \rightarrow \bar{s}$ , the short diagonal segments converge to the pole points.

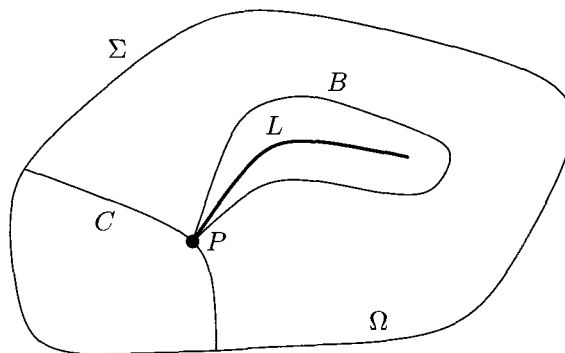


Fig. 29

### 8.3. Perturbing the spheres

LEMMA 8.4. *Suppose that  $s$  is as in Corollary 8.2. For  $j=0,1,2$  there are piecewise smooth embedded spheres  $\Sigma'_{j,s}$  such that*

- (1)  $I_{j,s}(\Sigma'_{i,s}) = \Sigma'_{j,s}$  and  $I_{j,s}$  interchanges the two components of  $S^3 - \Sigma'_{j,s}$ ,
- (2)  $\hat{C}_{j,s} \subset \Sigma'_{j,s}$ ,
- (3)  $\Sigma'_{i,s} \cap \Sigma'_{j,s} = \{P_{i,j,s}\}$ ,
- (4) the sequence  $\{(I_{j,s}I_{i,s})^n(\Sigma'_{j,s})\}$  shrinks to the point  $P_{i,j,s}$  for  $i \neq j$ .

*Proof.* We suppress the parameter  $s$ . With one change, the argument in the proof of Lemma 5.2 shows that  $\{I_i I_j(\Sigma_j)\}$  shrinks to a point. The one change is that one of the endpoints of  $L_n$  is no longer independent of  $n$ , but rather varies in a compact subset of  $\mathbf{C}$  which is independent of  $n$ . This change has no effect on the argument.

Let  $L_{ij} = \Sigma_i \cap \Sigma_j$ . Since  $L_{ij} \subset \Sigma_j$ , the sequence  $\{I_i I_j(L_{ij})\}$  shrinks to a point. Also  $I_i(L_{ij}) \cap L_{ij} = P_{ij}$ . Likewise for  $I_j$ . From this, it is easy to construct a topological ball  $B_{ij} \subset S^3$  such that

- (1)  $\{I_i I_j(B_{ij})\}$  shrinks to  $P_{ij}$ ,
- (2)  $L_{ij} \cap B_{ij} = P_{ij}$ ,
- (3)  $\partial B_{ij} - P_{ij}$  is smooth,
- (4)  $I_i(B_{ij}) \cap B_{ij} = I_j(B_{ij}) \cap B_{ij} = P_{ij}$ ,
- (5)  $\partial B_{ij} - P_{ij}$  is transverse to both  $\Sigma_i$  and  $\Sigma_j$ ,
- (6)  $\partial B_{ij} \cap \Sigma_i$  and  $\partial B_{ij} \cap \Sigma_j$  are embedded disks, contained respectively in hemispheres  $\Omega_i$  and  $\Omega_j$  of  $\Sigma_i$  and  $\Sigma_j$ ,

(7)  $\gamma_{ij} = \partial B_{ij} \cap \Sigma_i$  is a simple closed curve which bounds disks on both  $\Sigma_i$  and  $B_{ij}$ . Likewise for  $\gamma_{ji} = \Sigma_j \cap B_{ij}$ .

The ball  $B_{ij}$  is not smooth at  $P_{ij}$ . The cone point at  $P_{ij}$  has an extremely small angle, as shown schematically in Figure 29. We think of  $B_{ij}$  as being contained in a tiny

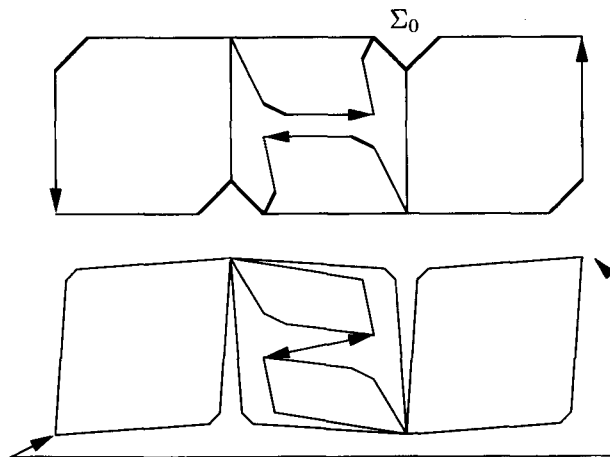


Fig. 30

neighborhood of  $L_{ij}$ . This is shown schematically in Figure 29.

Let  $\Delta_{ij}$  be the small disk on  $\Sigma_i$  bounded by  $\gamma_{ij}$ . Likewise define  $\Delta_{ji}$ . By construction,  $\gamma_{ij} \cap \gamma_{ji} = P_{ij}$ . In particular, there are disks  $\Delta'_{ij}$  and  $\Delta'_{ji}$  on  $B_{ij}$  such that  $\gamma_{ij} = \partial\Delta'_{ij}$  and  $\gamma_{ji} = \partial\Delta'_{ji}$  and  $\Delta'_{ji} \cap \Delta'_{ij} = P_{ij}$ .

We now explain how to modify  $\Sigma_0$ . The other cases are done by permuting the indices. Since  $s < \bar{s}$ , the segments  $L_{01}$  and  $I_0(L_{02})$  are disjoint. The same is true when 1 and 2 are switched. By choosing  $B_{0j}$  small enough, we can assume that  $\Delta'_{01} \cap I_0(\Delta'_{02}) = \emptyset$ . Likewise,  $\Delta'_{02} \cap I_0(\Delta'_{01}) = \emptyset$ . (A similar statement is automatically true for the  $\Delta$ -disks.) We create  $\Sigma'_0$  by replacing the four above-mentioned  $\Delta$ -disks by the corresponding  $\Delta'$ -disks. The modified spheres have all the desired properties.  $\square$

Figure 30 shows a schematic picture of our perturbation. In this picture, the four spheres adjacent to  $\Sigma_0$  have also been perturbed. The arrows indicate gluings which are not shown directly.

#### 8.4. Proof of Theorem 1.1

We have shown that it is possible, for  $s < \bar{s}$  sufficiently close to  $\bar{s}$ , to replace  $\Sigma_{j,s}$  by a perturbed sphere  $\Sigma'_{j,s}$ . The three spheres  $\Sigma'_{0,s}$ ,  $\Sigma'_{1,s}$  and  $\Sigma'_{2,s}$  retain all the properties of the original spheres, except that the stronger statement  $\Sigma'_{i,s} \cap \Sigma'_{j,s} = P_{ij,s}$  is true for all  $i \neq j$ .

Recall that  $\varrho_0(\Gamma)$  preserves the real slice  $X = \mathbf{R}^2 \cap \mathbf{CH}^2$ . Within  $X$ , a fundamental domain for this action is the ideal triangle bounded by the three geodesics  $\gamma_0, \gamma_1, \gamma_2$  fixed by the generating reflections. The orthogonal projection  $\Pi_X: \mathbf{CH}^2 \rightarrow X$  extends to  $S^3$ .

The three topological spheres

$$S_{j,0} = S^3 \cap \Pi_X^{-1}(\gamma_j)$$

intersect pairwise in a single point. The generators of  $\varrho_0(\Gamma)$  act on these spheres in the same way as the generators of  $\varrho_s(\Gamma)$  act on the spheres  $\Sigma'_{j,s}$ , constructed above. The topological conjugacy is obvious from here. The fact that all nested sequences of spheres shrink to points means that the conjugacy extends across the limit sets, without any problems.

It remains to analyze  $\Lambda_s$  and  $\Delta_s/\varrho_s(\Gamma)$ . Given our topological conjugacy, it suffices to consider the case  $s=0$ . The limit set  $\Lambda_0$  is obviously a circle. Let  $H_0$  be the index-2 subgroup of  $\varrho_0(\Gamma)$  consisting of even words. For each point  $x \in X$ , the fiber  $\Pi_X^{-1}(x) \cap S^1$  is a circle. From this it is easy to see that  $\Delta_0/H_0$  is a circle bundle over the thrice punctured sphere. All such bundles are trivial. Thus  $\Delta_0/\varrho_0(\Gamma)$  is doubly covered by  $S^1 \times S^2_3$ .

## 9. Proof of Lemma 8.1

The main idea in our proof of Lemma 8.1 is to replace the Heisenberg stereographic projection  $\mathbf{B}$  by a map  $\mathbf{B}_s$  which is adapted to the loxodromic element  $g_s$ . Once we have derived some basic properties of this map we will imitate Lemma 4.3 and Lemma 4.4.

### 9.1. Loxodromic stereographic projection

A basis of eigenvectors of  $g_s$  is given by

$$\widehat{O}_s = \Theta^{-1}(O_s), \quad \widehat{Q}_s = \Theta^{-1}(Q_s), \quad \widehat{E}_s = \lambda_s E_s^*, \quad \lambda_s \in \mathbf{R}. \quad (36)$$

All vectors are supposed to be affinely normalized. Here  $\Theta$  is as in equation (3).

Let  $X \in S^3 - E$ , with lift  $\tilde{X}$ . Define

$$\mathbf{B}_s(X) = (\Pi_s(X), \Lambda_s(X)), \quad (37)$$

$$\Pi_s(X) = \frac{\langle \widehat{X}, \widehat{E}_s \rangle}{\sqrt{\langle \widehat{X}, \widehat{O}_s \rangle \langle \widehat{X}, \widehat{Q}_s \rangle}}, \quad \Lambda_s(X) = \frac{1}{|x \langle \widehat{O}_s, \widehat{Q}_s \rangle|} \log \frac{|\langle \widehat{X}, \widehat{O}_s \rangle|}{|\langle \widehat{X}, \widehat{Q}_s \rangle|}. \quad (38)$$

These quantities are independent of the lift of  $X$ . One can consistently take a branch of the square root so that  $\Pi_s$  is globally defined.

LEMMA 9.1. *As  $s \rightarrow \bar{s}$ , the map  $\mathbf{B}_s$  converges, in the  $C^\infty$ -topology, to a map which agrees with  $\mathbf{B}$  up to composition with some map  $(z, t) \rightarrow (\lambda z, At)$  for  $\lambda \in \mathbf{C}^*$  and  $A \in \mathbf{R}^*$ .*

*Proof.* Recall that  $g_{\bar{s}}$  stabilizes the pair  $(E_0, P_0)$ . Let  $\widehat{P}_0$  be the affinely normalized lift of  $P_0$ , and let  $\widehat{E}_0$  be the affinely normalized lift of the vector polar to  $E_0$ . Note that

$\widehat{E}_0$  and  $\widehat{P}_0$  are multiples of the similarly named vectors from equation (19). The points  $\widetilde{O}_s$  and  $\widetilde{Q}_s$  converge to  $\widehat{P}_0$ , and  $\widetilde{E}_s$  converges smoothly to  $\widehat{E}_0$ . Note that  $Q_s$  does not converge to a multiple of  $\widetilde{Q}_0$ , the vector used in equation (19). Define

$$\hat{J}_s = \widehat{O}_s - \widehat{Q}_s, \quad \widehat{U}_s = \hat{J}_s / \|\hat{J}_s\|, \quad \widehat{U} = \lim_{s \rightarrow \bar{s}} \widehat{U}_s. \quad (39)$$

By construction,  $\widehat{U}$  is tangent to the chain  $E_0$  at  $P_0$ , and contained in the complex line which contains  $E_0$ . Since  $E_0$  is transverse to the contact structure, we have  $\langle \widehat{P}_0, \widehat{U} \rangle \neq 0$ . The points  $P_0$  and  $Q_0$  are diametrically opposed on  $E_0$ , because  $R_0$  is an isometry which interchanges the two components of  $E_0 - P_0 - Q_0$ . Since  $\widehat{P}_0 - \widehat{Q}_0 = P_0 - Q_0$ , there is some  $K_1 \in \mathbf{R}$  such that

$$iK_1 \widehat{U} = \widehat{Q}_0 - \widehat{P}_0. \quad (40)$$

Let  $W$  be an open subset whose closure is contained in  $S^3 - E_0$ . Let  $X \in W$  be a point with lift  $\widetilde{X}$ . The convergence above gives

$$\lim_{s \rightarrow \bar{s}} \Pi_s(X) = \frac{\langle \widetilde{X}, \widehat{E}_0 \rangle}{\langle \widetilde{X}, \widehat{P}_0 \rangle}. \quad (41)$$

When  $\Pi_s$  is considered as a function of  $W$ , the convergence takes place in the smooth topology, because all vectors vary smoothly.

Below we will show that there is a constant  $K_2 \in \mathbf{R}$  such that

$$\lim_{s \rightarrow \bar{s}} \Lambda_s = K_2 \operatorname{Im} \frac{\langle \widetilde{X}, \widehat{V} \rangle}{\langle \widetilde{X}, \widehat{P}_0 \rangle}, \quad \widehat{V} = -iK_1 \widehat{U}. \quad (42)$$

Once again, the nature of our formulas is such that the convergence of the corresponding functions takes place in the smooth topology.

Combining equations (40), (41) and (42) we get

$$\mathbf{B}_\infty = \pi \circ \Theta \circ M_\infty, \quad M_\infty(X) := (\langle \widetilde{X}, \widehat{E}_0 \rangle, \langle \widetilde{X}, K_2 \widehat{Q}_0 \rangle, \langle \widetilde{X}, \widehat{P}_0 \rangle). \quad (43)$$

Here  $\Theta$  and  $\pi$  are as in equations (3) and (5). The vectors used in this last equation are all multiples of the ones used in equation (19).

To finish the proof, we derive equation (42). Since  $\langle \widehat{Q}_s, \widehat{Q}_s \rangle = 0$ , we get

$$\Lambda_s(X) = \frac{\log |1 + \|\hat{J}_s\| |z_1(s)|}{\|\hat{J}_s\| |z_2(s)|}, \quad z_1(s) = \frac{\langle \widetilde{X}, \widetilde{U}_s \rangle}{\langle \widetilde{X}, \widetilde{Q}_s \rangle}, \quad z_2(s) = \langle \widehat{Q}_s, \widehat{U}_s \rangle. \quad (44)$$

Writing  $z_1 = x_1 + iy_1$  we have

$$\log |1 + \|\hat{J}_s\| |z_1(s)| = \frac{1}{2} \log(1 + 2\|\hat{J}_s\| |x_1(s)| + \|\hat{J}_s\|^2 |z_1(s)|^2). \quad (45)$$

If we define

$$\theta(s) = \frac{x_1(s)}{|z_2(s)|} + \frac{\|\hat{J}_s\| |z_1(s)|^2}{2|z_2(s)|}, \quad \eta(s) = 2\|\hat{J}_s\| x_1(s) + \|\hat{J}(s)\|^2 |z_1(s)|^2, \quad (46)$$

then, as long as  $|\eta(s)| < 1$ , we can expand out equation (45) in a Taylor series:

$$\Lambda_s(X) = \theta(s) \left(1 - \frac{1}{2}\eta(s) + \frac{1}{3}\eta^2(s) - \frac{1}{4}\eta^3(s) + \dots\right). \quad (47)$$

Since  $\lim_{s \rightarrow \bar{s}} \hat{J}_s \rightarrow 0$  and  $\lim_{s \rightarrow \bar{s}} z_2(s) = \langle \hat{P}_0, \hat{U} \rangle = \zeta \neq 0$  we get

$$\lim_{s \rightarrow \bar{s}} \Lambda_s = \lim_{s \rightarrow \bar{s}} \theta(s) = K_3 \lim_{s \rightarrow \bar{s}} x_1(s) = K_3 \operatorname{Re} \frac{\langle \tilde{X}, \hat{U} \rangle}{\langle X, \hat{P}_0 \rangle} = K_2 \operatorname{Im} \frac{\langle \tilde{X}, \hat{V} \rangle}{\langle X, \hat{P}_0 \rangle}. \quad (48)$$

Here  $K_3 = 1/|\zeta|$ . □

**LEMMA 9.2.** *If  $\gamma$  is an  $\mathbf{R}$ -arc which intersects  $E_{0,s}$  in points which are harmonic conjugates with respect to  $P_{0,s}$ , then  $\mathbf{B}_s(\gamma) = (S - \{0\}) \times \{r\}$ . Here  $S$  is a line segment through 0.*

*Proof.* Writing everything out in the basis  $(\tilde{O}_s, \tilde{Q}_s, \tilde{E}_s)$ , we see that  $\mathbf{B}_s$  conjugates the stabilizer subgroup of  $P_{0,s}$  to the isometries of  $\mathbf{C} \times \mathbf{R}$  which preserve  $\{0\} \times \mathbf{R}$ . There is one element in the stabilizer of  $P_{0,s}$  which interchanges its endpoint and has  $\gamma$  as its fixed point set.  $\mathbf{B}_s$  conjugates this element to an isometry of  $\mathbf{C} \times \mathbf{R}$ , and this isometry must be an order-2 rotation about a line of the form  $S \times \{r\}$ . Hence, this line contains  $\mathbf{B}_s(\gamma)$ . □

**LEMMA 9.3.** *There is a set  $K_s \subset S^3$  such that*

(1)  $\mathbf{B}_s$  is a diffeomorphism from  $S^3 - K_s$  onto its image,

(2) the differential  $d(\pi_{\mathbf{C}} \circ \mathbf{B}_s)$  is nonsingular and complex linear on each complex line tangent to a point of  $S^3 - K_s$ .

$K_s$  shrinks to  $P_0$  as  $s \rightarrow \bar{s}$ .

*Proof.* The map  $\Pi = \pi \circ \Theta$  extends to a holomorphic mapping of an open subset of  $\mathbf{C}^2$ . Hence,  $d\Pi$  is automatically complex analytic on complex tangencies.  $d\Pi$  is nonsingular on the complement of a vanishingly small set, by Lemma 3.9. □

## 9.2. End of the proof

Let  $\Sigma_{1,s}^*$  and  $\Sigma_{2,s}^*$  be the hemispheres of  $\Sigma_{1,s}$  and  $\Sigma_{2,s}$  which share the common spine  $(E_{0,s}, P_{0,s})$ . Let  $\Sigma_{j,s}^{**}$  be the other hemisphere of  $\Sigma_{j,s}$ . Let  $\Sigma_j^*$  and  $\Sigma_j^{**}$  be the corresponding hemispheres of the parabolic hybrid sphere  $\Sigma_j$ . Let  $\varepsilon$  be so small that  $|s - \bar{s}| < \varepsilon$  implies:

(1) There are no complex lines tangent to  $\Sigma_{j,s}$  at points in  $U_\varepsilon$ . This is possible by Lemma 3.10.

(2) Referring to Lemma 9.3, we have  $U_\varepsilon \subset K_s$ .

Define

$$R_{j,s,\varepsilon} = \Sigma_{j,s}^{**} \cap U_\varepsilon. \quad (49)$$

Since  $\Sigma_{j,s}$  is a smooth surface, with uniform bounds from above on its normal curvatures, we can take  $\varepsilon$  so small that  $R_{j,s,\varepsilon}$  is an embedded disk.

LEMMA 9.4. *For  $\varepsilon$  sufficiently small,*

$$\xi \circ \mathbf{B}_s(\partial R_{1,s,\varepsilon}) \cap \xi \circ \mathbf{B}_s(\partial R_{2,s,\varepsilon}) = \xi \circ \mathbf{B}_s(P_{12,s}).$$

*Proof.* We have

$$\partial R_{j,s,\varepsilon} = (\partial U_\varepsilon \cap \Sigma_{j,s}^{**}) \cup (U_\varepsilon \cap \widehat{C}_{j,s}).$$

The arc  $\xi \circ \mathbf{B}_s(U_\varepsilon \cap \widehat{C}_{j,s})$  is the graph of a function  $f_{j,s}$ , defined in a neighborhood of  $0 \in \mathbf{R}/2\pi\mathbf{Z}$ . Since  $R_0$  interchanges  $\Sigma_{1,s}$  and  $\Sigma_{2,s}$ , as in the parabolic case, we have  $f'_{1,s}(0) = f'_{2,s}(0)$ . By Lemma 3.9, the function  $f_{j,s}$  converges smoothly to the function  $s_j$ , used in the proof of Lemma 4.3. Hence,  $f''_{1,s}(t) > 0$  and  $f''_{2,s}(t) < 0$  for  $t$  sufficiently close to 0. Therefore

$$\xi \circ \mathbf{B}_s(\widehat{C}_{1,s} \cap U_\varepsilon) \cap \xi \circ \mathbf{B}_s(\widehat{C}_{2,s} \cap U_\varepsilon) = \xi \circ \mathbf{B}_s(P_{12,s}).$$

From Lemmas 4.3 and 4.4 we have

$$\begin{aligned} \xi \circ \mathbf{B}(\widehat{C}_1 \cap U_\varepsilon) \cap \xi \circ \mathbf{B}(\Sigma_2^{**} \cap \partial U_\varepsilon) &= \emptyset, \\ \xi \circ \mathbf{B}(\widehat{C}_2 \cap U_\varepsilon) \cap \xi \circ \mathbf{B}(\Sigma_1^{**} \cap \partial U_\varepsilon) &= \emptyset, \\ \xi \circ \mathbf{B}(\Sigma_2^{**} \cap \partial U_\varepsilon) \cap \xi \circ \mathbf{B}(\Sigma_1^{**} \cap \partial U_\varepsilon) &= \emptyset. \end{aligned}$$

By continuity, the analogous formula is true for  $s$  sufficiently close to  $\bar{s}$ .  $\square$

Let  $X^\circ$  be the interior of the set  $X$ . Lemma 8.1 is an immediate consequence of the preceding result, and the following result:

LEMMA 9.5. *For  $\varepsilon$  sufficiently small, and  $|s - \bar{s}| < \varepsilon$ , the set  $\xi \circ \mathbf{B}_s(R_{j,s,\varepsilon}^\circ)$  is contained in the interior of the compact region bounded by  $\xi \circ \mathbf{B}_s(\partial R_{j,s,\varepsilon})$ .*

*Proof.* We imitate the proof of the Dollar Sign Lemma. We define the *inward radials* of  $R^\circ$  to be arcs of the form  $\pi_{\mathbf{C}} \circ \mathbf{B}_s(\alpha)$ , where  $\alpha$  is an  $\mathbf{R}$ -arc foliating  $R^\circ$ . We have arranged that there are no contact planes tangent to  $R^\circ$ . We have also established Lemma 9.2 and Lemma 9.3.



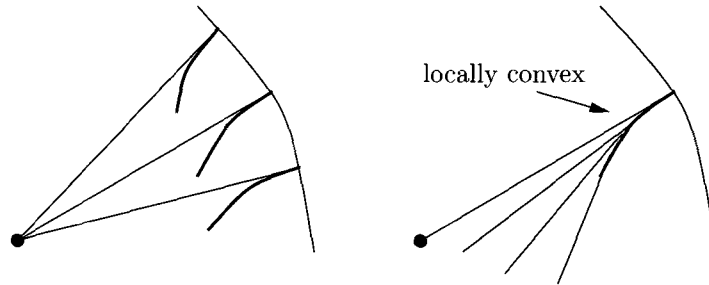


Fig. 31

It suffices to prove that the fibers of  $\xi \circ \mathbf{B}_s$  are transverse to  $R_{j,s,\varepsilon}^o$ . If this is false then there is a segment through the origin which is tangent to an inward radial of  $R^o$  at an interior point.

The inward radials of  $R^o$  are open arcs. One endpoint of each inward radial is contained on the  $\mathbf{C}$ -arc  $\pi_{\mathbf{C}} \circ \mathbf{B}_s(\widehat{C}_{j,s})$ . The same argument as in Lemma 4.4 shows that the tangent lines to inward radials at these endpoints contain the origin, as shown in Figure 31.

In the parabolic case, the inward radial of  $\pi_{\mathbf{C}} \circ \mathbf{B}(\Sigma_j)$ , whose endpoint is  $\pi_{\mathbf{C}} \circ \mathbf{B}(P_{12})$ , is locally convex at  $P_{12}$ . By Lemma 3.9 and continuity, the same statement is true at all points of all inward radials of  $R^o$ , as long as  $\varepsilon$  is chosen small enough. By convexity, the tangent lines to a fixed inward radial of  $R^o$ , at distinct points, cannot both contain the origin. Since the tangent line at one endpoint contains the origin, the tangent line at any other point does not contain the origin.  $\square$

### References

- [E] EPSTEIN, D. B. A., Complex hyperbolic geometry, in *Analytical and Geometric Aspects of Hyperbolic Space* (Warwick and Durham, 1984), pp. 93–111. London Math. Soc. Lecture Note Ser., 111. Cambridge Univ. Press, Cambridge–New York, 1987.
- [FZ] FALBEL, E. & ZOCCA, V., A Poincaré’s polyhedron theorem for complex hyperbolic geometry. *J. Reine Angew. Math.*, 516 (1999), 133–158.
- [G] GOLDMAN, W. M., *Complex Hyperbolic Geometry*. Oxford Math. Monographs. Oxford Univ. Press, New York, 1999.
- [GKL] GOLDMAN, W. M., KAPOVICH, M. & LEEB, B., Complex hyperbolic surfaces homotopy equivalent to a Riemann surface. To appear in *J. Geom. Anal.*
- [GP] GOLDMAN, W. M. & PARKER, J. R., Complex hyperbolic ideal triangle groups. *J. Reine Angew. Math.*, 425 (1992), 71–86.
- [GuP] GUSEVSKII, N. & PARKER, J. R., Complex hyperbolic quasifuchsian surfaces. Preprint, 1999.
- [KR] KORÁNYI, A. & REIMANN, H. M., Quasiconformal mappings on the Heisenberg group. *Invent. Math.*, 80 (1985), 309–338.

- [S] SCHWARTZ, R., Ideal triangle groups, dented tori and numerical analysis. To appear in *Ann. of Math.*
- [Th] THURSTON, W. P., *Three-Dimensional Geometry and Topology*. Princeton Math. Ser., 35. Princeton Univ. Press, Princeton, NJ, 1997.
- [To] TOLEDO, D., Representations of surface groups in complex hyperbolic space. *J. Differential Geom.*, 29 (1989), 125–133.

RICHARD EVAN SCHWARTZ  
Department of Mathematics  
University of Maryland  
College Park, MD 20942  
U.S.A.  
res@math.umd.edu

*Received May 17, 1999*

*Received in revised form December 15, 1999*